EPSC2017

SB2 abstracts

EPSC Abstracts
Vol. 11, EPSC2017-79, 2017
European Planetary Science Congress 2017

New Catalogue of One-Apparition Comets discovered in the years 1901–1950. Part II

Małgorzata Królikowska (1), Sławomira. Szutowicz (1), Ryszard Gabryszewski (1), Hans Rickman (1,2), Krzysztof Ziołkowski (1) and Eduard M. Pittich (3)
(1) Space Research Centre of the Polish Academy of Sciences, Bartycka 18A, 00-716 Warsaw, Poland (mkr@cbk.waw.pl)
(2) Department of Physics and Astronomy, Uppsala University, Box 516, SE-75120 Uppsala, Sweden
(3) Astronomical Institute of the Slovak Academy of Sciences, 845 04 Bratislava, The Slovak Republic

Abstract

First part of this Catalogue includes 38 Oort spike comets discovered in the first half of 20th century ([1]). Here, we present almost complete orbital results of the second part of the new catalogue of near-parabolic comets having orbital periods greater than 200 yr and original semimajor axes shorter than 10 000 au according to the latest edition of the Marsden and Williams Catalogue of Cometary Orbits (2008, hereafter MW08). This sample consists of about 50 comets having original semimajor axes shorter than 10 000 au, where in the case of eight comets their orbits are quality class worse than 2 in MW08 (original $1/a$ is not given there in such cases), and of 34 comets with parabolic orbits given in MW08 ($e = 1$ was assumed for these objects). New orbit recalculations generally give orbits of better quality, what is clearly visible within the subsample of the worst originally determined orbits. For at least half of the analysed comets from the 'parabolic' group of orbits it turns out that their eccentricities:
(i) are determinable at a comparable level of accuracy as in the case of eight orbits of class < 2 mentioned above,
(ii) suggest that their aphelia lie within the inner Oort Cloud region.
This investigation is a part of long-lasting project (Warsaw Catalogue of Near-Parabolic Comets) aimed at deriving the cometary orbits using the homogeneous methods and solar system model, and dynamical models of cometary motion that take into account the non-gravitational accelerations.

Acknowledgements

This investigation was partially supported from the project 2015/17/B/ST9/01790 founded by National Science Centre in Poland.

References

[1] Królikowska, M., Sitarski, G., Pittich, E. M., Szutowicz, S., Ziołkowski, K., Rickman, H., Gabryszewski, R., and Rickman, B.: New catalogue of one-apparition comets discovered in the years 1901-1950. I. Comets from the Oort spike, A&A, Vol. 571, A63, 2014.

EPSC Abstracts
Vol. 11, EPSC2017-81, 2017
European Planetary Science Congress 2017

Capture of Small Bodies After Tidal Disruption

A. Ershova (1,2), Yu. Medvedev (1)
(1) Institute of Aplied Astronomy of RAS, St. Petersburg, Russia, (2) Saint Petersburg State University, St. Petersburg, Russia, (eap@iaaras.ru / Fax: ++7 (812) 275-1119)

Abstract

The subject of the current work is the phisical and dynamical evolution of the small comets group formed by tidal disruption of the protocomet while passing near the large body (Sun, Jupiter). The equations of motion were integrated numericaly. In case of the Sun the evolution of the sun-grazing orbits were discussed and the typical lifetime of such comets was estimated. Nongravitational acceleration and the size reduction of fragments due to sublimation were taking into account.

1. Introduction

A long-standing problem in cometary astronomy is the mechanism of capture of Halley-type comets from near-parabolic flux. There is the difficulty of explaining the apparent over abundance of Jupiter-family comets compared with predictions based on capture from the observed near-parabolic comets flux. In this paper we try to solve these problems by Opics capture of icy fragments (the capture by the massive body after tidal disruption of large protocomet). The large comet could be disrupted by the tidal forces during the close approach to the Sun or a giant planet. This is one of the main hypothesis of the Kreutz comet group formation [4]. In such case the cloud of comet fragments of different sizes is formed. Their further trajectories can be described as independent. The fragments' positions are very close to each other in the perihelion. However the comet cloud stretches sufficiently while moving to aphelion. The orbits of the fragments can evolve in different ways under influence of the planets' gravitational perturbations and the sublimation jet force.

The evolution of near-parabolic orbits was previously discussed by researchers [2]. It is noticed that the high-eccentricity orbits are more likely to evolve in the inner regions of the Solar System if they had initially small perihelion distance. The sun-grazing orbits are interesting as an extreme case of such orbits. Besides the close approach to the Sun is typical for many of the asteroids approaching the Earth [1]. So the evolution of sun-grazing orbits can be considered as a potential source of near-Earth objects.

2. Orbit evolution

We considered two model problems, namely, the disruption near the Sun and near Jupiter. The differential equations of motion were integrated numerically. The planets' motion was considered as nonperturbed in both cases.

2.1. Disruption near the Sun

In case of the Sun the protocomet moved on the near-parabolic orbit with the eccentricity equal to 0.99993 and the semi-major axis equal to 100 AU. The disruption took place in the perihelion in the distance of 0.007 AU from the Sun. The fragments which appeared closer to the Sun passed to less elliptical orbits because they kept the speed the parent body had.

The sublimation acceleration was calculated according to the Marsden formula[3]. The comets were considered as ice spheres. The change in size of the comet was taken into account.

Without close approaches to planets the complete combustion of a comet on sun-grazing orbit takes several thousands of years.

Also we considered the occasion when the comet cloud after disruption at the perihelion is passing close to Jupiter. It should be noted that if the initial size of the cloud was 100 km it would be about 0.1 AU while crossing the Jupiter's orbit. In this case the gravitational influence of Jupiter was enough to capture some of comets to the low-eccentricity orbits.

2.2 Disruption near Jupiter

In case of Jupiter large protocomet moved on the hyperbolic orbit with perihelion in the close vicinity of Jupiter. The disruption occured on the distance of

0.0005 AU from the planet. We modeled the different configurations in terms of the Sun-Jupiter-comet position. The 100 km cloud after passing the Jupiter sphere of influence was stretched in size up to 0.02 AU.

Part of these comets moved on a such distance from the Sun so the sublimation effect was small or even neglectable. First of all it means that comets does not burn down quickly and can exist for cosmogonic time.

3. Summary and Conclusions

The main result of this work is the cloud of the protocomet's fragments become very dispersed right after disruption. The sun-grazing orbits are not likely to evolve in the inner regions of the Solar System because the sun-grazers burn down too fast.

However a giant protocomet disrupted near the Jupiter might be a source of the small bogies on long existing orbits.

Acknowledgements

The work was performed with support of Russian Science Foundation grant. (No 16-12-00071).

References

[1] Brett Gladman. Author links open the author workspace.Patrick Michel. Author links open the author workspace.Christiane Froeschlé : The Near-Earth Object Population, Icarus, Vol. 146, pp. 176-189, 2000

[2] Emel'yanenko V.V. and Bailey, M.E.: Capture of Halley-type comets from the near-parabolic flux, Mon. Not. R. Astron. Soc., Vol. 298, pp. 212-222, 1998.

[3] Marsden B.G. and Sekanina Z.: Comets and nongravitational forces. V., The Astronomical Journal, Vol. 78, n. 2, 1973

[4] Opic E.J. : sun-grazing comets and tidal disruption, The Irish Astronomical Journal, Vol. 7, n. 5, 1966

EPSC Abstracts
Vol. 11, EPSC2017-101, 2017
European Planetary Science Congress 2017

Analysis of photometric, spectroscopic, and polarimetric observations of five distant comets

O. Ivanova (1,2), V. Afanasiev (3)
(1) Astronomical Institute of the Slovak Academy of Sciences, SK-05960 Tatranská Lomnica, Slovak Republic, (oivanova@ta3.sk/ Fax: +421524467656) (2) Main Astronomical Observatory of the National Academy of Sciences of Ukraine, Akademika Zabolotnoho 27, 03143 Kyiv, Ukraine (3) Special Astrophysical Observatory of the Russian Academy of Sciences, Nizhnij Arkhyz, Karachai Cherkessian Republic, 369167, Russia (vafan@sao.ru/ Fax: +78787846315)

Abstract

Photometric, polarimetric, and spectroscopic observations of five nearly parabolic comets at heliocentric distances greater than 4 AU were performed. No molecular emission was observed for any studied comet and the entire cometary activity in all cases was attributed to dust production. Upper limits of the gas production rates for the main neutral molecules in the cometary comae were calculated. The derived values of dust apparent magnitudes were used to estimate the upper limit of the geometric cross-section of cometary nuclei. The maps of intensity and linear polarization over the coma are derived. The linear polarization of distant comets with a high level of activity is the first ever measured at the heliocentric distances larger than 4 AU.

Introduction

Physical nature of comets is known mainly from the observations of bright comets close to the Earth and the Sun (typically 1−2 AU). A few of the Jupiter, Neptune family comets and Kuiper-Belt objects have been investigated with space experiments, while observations at large heliocentric distances (more than 4 AU) are still scarce and episodic, thereby not covering very important stage of the development of cometary activity.

The reasons for the activity of distant comets can not be interpreted by the available theory of the origin of the comets, there is no generally recognized explanation for this phenomenon. Sublimation of more volatiles than water ice, for example, CO, CO_2, N_2, can serve as a probable explanation of the problem. Condensation of these gases on dust grains, or by their capture by condensed molecules of water, is possible only at temperature of an environment which does not exceed 25-30 K. Such temperature conditions could be realized or in an interstellar cloud from which the Solar system was originated, or at early stage of the Solar System formation.

1. Observations

We have started a comprehensive program of polarimetric, photometric, and spectral investigations of active distant comets (or without noticeable activity) with the focal reducer SCORPIO-2 [1] attached at prime focus of 6-m telescope BTA (Special Astrophysical Observatory, Russia). We performed broad-band photometry, polarimetric imaging and long-slit spectroscopy of C/2011 S1 (LINEAR), C/2011 R1 (LINEAR), C/2014 A4 (SONEAR), C/2013 V4 (Catalina), and C/2011 KP36 (Spacewatch) in the visible wavelength range at phase angle from 4.9° to 14°, when the comets were at the heliocentric distances from 3.2 to 6 au.

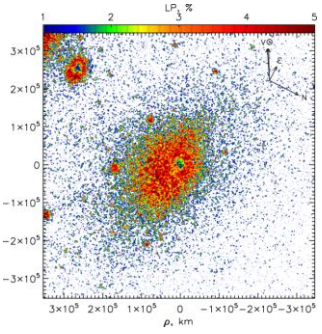

Figure 1: Polarization map of comet C/2011 KP36 (Spacewatch) on November 25, 20165. The arrows show the directions to the Sun, North, East, and motion of the comet. The heliocentric distance off the comet r=5.06 au and phase angle α=9.5°

Our observations of comets at large heliocentric distances revealed the occurrence of a well-observable dust cloud near the cometary nuclei, but we did not detect any gas. The results of photometry

investigation of five distant comets presented here show activity properties that are typical for new comets. The Afρ value obtained and the dust production for our objects are of the same order as those measured for most of dynamically new and long period comets.

Summary and Conclusions

Distant comets show considerable levels of activity not only within a zone of water sublimation (up to 3 AU) but also at heliocentric distances far exceeding this limit. Molecular emissions are not detected in the observed cometary spectra. The cometary comae display the degree of linear polarization within the range of about (−2 ÷ −2.5)% and (−2.5 ÷ −3.5)%, respectively. These values are higher (in absolute value) than that (about −1.5%) typical of close to the Sun comets.

Acknowledgements

The observations with the 6-m BTA telescope were conducted with the financial support of the Ministry of Education and Science of the Russian Federation (agreement No. 14.619.21.0004, project ID RFMEFI61914X0004). O. Ivanova thanks the SASPRO Programme for the financial support.

References

[1] Afanasiev, V.L. Moiseev, A.V. 2011. Scorpio on the 6 m Telescope: Current State and Perspectives for Spectroscopy of Galactic and Extragalactic Objects. Astrophys. Bull. 20, 363–370.

.

EPSC Abstracts
Vol. 11, EPSC2017-159, 2017
European Planetary Science Congress 2017

A study of the effects of faint dust comae on the spectra of asteroids

E. Rondón (1), J. Carvano (1) and S. Lorenz-Martins (2)
(1) Observatório Nacional, Rio de Janeiro, Brazil. (2) Observatório do Valongo, Rio de Janeiro, Brazil (erondon@on.br)

Abstract

The presence of dust comae on asteroids and centaurs is a phenomenon that became accepted in the last decades and which challenges the traditional definitions of asteroids and comets. A possible way of improving the chances of discovery of Active Asteroids is to use large multi-colour surveys or catalogs, like SDSS Moving Object Catalog. In this work we analyze the effects of faint dust comae on asteroid spectra and then use it to investigate the effects that a faint dust comae would have over the spectrum, magnitude, and radial profile of asteroids.

1. Introduction

Seventeen asteroids of the Main Belt and three Near Earth Asteroids have shown cometary activity. These objects have been called Active Asteroids (AA) (Jewitt, 2012). The physical source of their activity can be diverse; among the possible causes are collisional and volatile sublimation processes. The detection of AA is determined by the presence of a coma in its photometry, nevertheless this coma could be so faint that it would be very difficult to detect it. In this work we study the influence of a faint coma over the asteroid in the spectra. This has already been suggested by Carvano et al. (2008) to the observe the atypical spectrum of the asteroid (5201) Ferraz-Mello and modeled by Carvano & Lorenz-Martins (2009) from which they were capable to produce a reflectance increase in shorter wavelengths, and shows that presence of a faint coma produces an unusual reflectance.

2. Summary and Conclusions

In our model, we study more realistic distribution of particle in comae formed by sublimation or collisional ejection. This allowed us to study different parameters that influence the formation of coma. The size distribution of particles in the coma, their optical properties, and the physical processes responsible for creating such distribution are complex and depend on many variables such that all this will influence the obtained result. From our model it is evident that a coma in the asteroid (Figure 1a-b) produces changes in the observed spectra (Figure. 1c), increase in the brightness (Figure. 1d) and modify the radial profile (Figure. 3). In the case of the spectra, other processes can also affect this in a similar way. However, one possible indicative of presence of coma would be the relative increase in the reflectance at the bluer end of the spectrum.

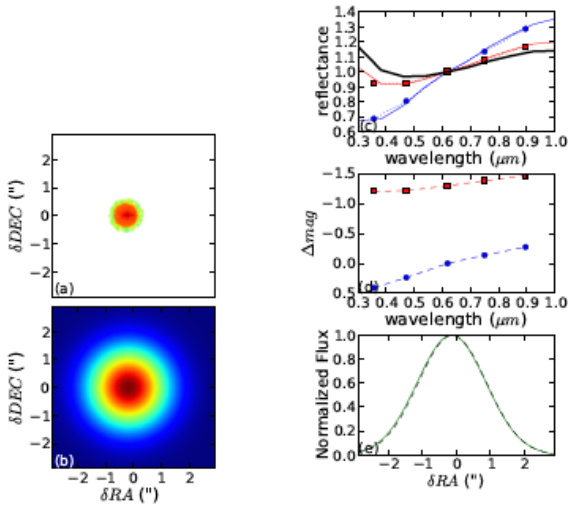

Figure 1: Reflectance normalized modeled at the central wavelength of the r filter for a total mass in the coma of $M_c = 10^6$kg and a phase angle of g = 6º, seen 3 days after ejection. (a) Brightness projected at the plane of sky; the intensity is shown with a logarithm colour map; (b) the same result, convolved with a PSF with 1 arcsec FWHM, shown using a linear colourmap. (c) Reflectance normalized at the central wavelength of the r filter. The reflectance

spectra of the asteroid without coma is shown in blue, the reflectance at the SDSS filters (obtained through convolution of the reflectance spectra with the filter band passes) are show as circles and connected with a dotted line. The reflectance spectra of only the coma is shown in black and the combination of the spectra of the asteroid and the coma is shown in red, with the reflectance at the SDSS filters shown as squares. ; (d) Difference of magnitudes between the asteroid (blue circles) and the asteroid in the presence of the coma (red squares), with the asteroid magnitude at the r filter as reference. (e) Radial profile of the normalized Flux at r filter convolved with a 1 arcsec PSF.

In conclusion, the model presented in this work allows a finer understanding of the observational consequences of faint comae that might be present around minor bodies of the Solar System. In this work is showed that often the sole indicative of the existence of such faint coma would be changes in the observed spectra. Even so, spectral variations alone cannot be considered proof of such phenomena. Instead, the type of spectral variations highlighted here can be use to refine the list of potential AA so that confirmations of the presence of comae through careful photometric monitoring of the candidates to identify sudden increases in the magnitude, and through efforts to detect extended profiles on images of those bodies.

Acknowledgements

The authors would like to thank T. Roush for providing the optical constants of the Tagish Lake meteorite. J.M.C would like to thank CNPq and CAPES for supporting this work through diverse fellowships and grants. E.R. would like to thank to CNPq for supporting his work with a PhD fellowship.

References

[1] Jewitt D. (2012) *AJ. 143,* 66.

[2] Carvano J. et al. (2008) *A&A., 489,* 811-817.

[3] Carvano J. and Lorenz-Martin, S. (2009) Proceedings of the International Astronomical Union, 5, 223-226.

EPSC Abstracts
Vol. 11, EPSC2017-170-1, 2017
European Planetary Science Congress 2017

Investigation of the comet 29P/Schwassmann-Wachmann 1 at the SOAR telescope

O. V. Ivanova (1,2), I. V. Luk'yanyk (3), E. Picazzio (4), Oscar Cavichia de Moraes (5), Amaury Augusto de Almeida (4) and S. M. Andrievsky (6)
(1) Astronomical Institute of the Slovak Academy of Sciences, Slovak Republic (oivanova@ta3.sk/ Fax: +42-152-446-76-56)
(2) Main Astronomical Observatory of the National Academy of Sciences of Ukraine, Ukraine
(3) Astronomical Observatory, Taras Shevchenko National University of Kyiv, Ukraine
(4) Universidade de São Paulo, Instituto de Astronomia, Geofísica e Ciências Amosfércas, Brasil
(5) Instituto de Física e Química, Universidade Federal de Itajubá, Brasil
(6) Astronomical Observatory, Odessa National University, Ukraine

Abstract

We carried out photometric and spectroscopic observations of comet 29P/Schwassmann–Wachmann 1 at the SOAR 4.1-meter telescope (Chile) on August 11, 2016. The spectra revealed the presence of $CO+$ and N_2^+ emissions in the cometary coma at a distance of 5.9 AU from the Sun. The ratio $[N_2^+]/[CO^+]$ within the projected slit be of 0.01. The images obtained through BVRI filters showed a faint, dust coma. We estimated a color index and a color excess for the comet. The parameter $Af\rho$, which is used as an indicator of a cometary activity, was measured. We also investigated the morphology of the comet using digital filters and found two jets in the coma.

1. Introduction

Small bodies with orbits beyond that of Neptune are of interest because they must have undergone minimal changes since the Solar System formation. The equilibrium temperature ($\leqslant$140 K) at these distances is too low to ensure a significant level of physical activity caused by the sublimation of water ice. As of today, the active centaur 29P/Schwassmann-Wachmann 1 (SW1) is still the most interesting and studied distant object. In this work we carried out investigation of comet SW1 at the SOAR 4.1-meter telescope. The comet was observed at the heliocentric distance of 5.9 AU, and showed low activity and faint coma.

2. Observations

Photometric and spectrophotometric observations were made at the SOAR 4.1 m telescope in Cerro Pachón - Chile during August 11, 2016. The Goodman imaging/spectrograph was used with a 600 l/mm grid, which provides for the spectroscopic mode a reciprocal dispersion of 0.065 nm/pixel and, using a 1.68 arcsec slit width, a spectral element resolution of 0.73 nm. The SOAR Goodman spectrograph blue camera features one 4096 x 4096 pixel Fairchild CCD and a 7.2 arcsec in diameter field of view in the imaging mode. The photometry was done with Bessel BVRI filters. The seeing was stable during the night, with a mean value of 0.8 arcsec FWHM. The cometary spectra were acquired with 10 exposures, which were also co-added to increase the final signal-to-noise ratio. The spectrophotometric standard stars LTT 9491 was observed with a long slit of 3 arcsec width, allowing a more precise flux calibration. Data reduction was performed using the IRAF package, following the standard procedure for ccd reduction, i.e. correction of bias and flat-field. The spectral images were extracted and calibrated in wavelength and flux. Atmospheric extinction was corrected through mean coefficients derived for the CTIO observatory.

3. Results

From the spectral and photometrical data, it was possible to obtain the distribution of energy in wavelength, to identify the molecular emissions, and to estimate the dust color and dust production rate (like [1]). The comet SW1 shows long-term outburst activity in the form of dust jets, which can be considered typical for this comet. To select the weak contrast structures (jets) in the images of the dust coma, we used the special software Astroart, which is provided with a number of digital filters. To eliminate false details, each of the filters was separately applied to each image. After this filtering we selected jets structures.

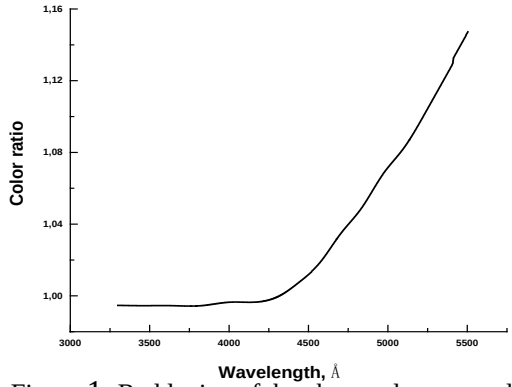

Figure 1: Reddening of the observed spectra relative to the solar spectrum

Using the median filter with wide window, we obtained a smoothed curve that reproduces spectral dependence of the solar radiation scatter efficiency caused by the cometary dust particles. The result is given in Figure 1, and one can see that there is a nonlinear increase with the wavelength of the scattering efficiency. For our observations the normalized reflection ability:

$\boldsymbol{S'(\lambda_1, \lambda_2)}$ = 11,31 ± 0,04% for the range 4430-5260 Å

The strongest features seen along the whole observed spectral window are the CO^+ bands from the comet tail. The lines (2,0), (3,0), (2,0), (1,0), (5,1), (3,1) , (2,1), (4,2), (3,2), (0,0), and (1, 1) of the vibrational transitions band system ($A^2\Pi$–$X^2\Sigma$) of the CO^+ are clearly seen in Figure 2. Two weak bands, (0,1) and (1,2) from the ($B^2\Sigma$–$A^2\Pi$) system (Baldet–Johnson) of the CO^+ ion, were detected as well. The N_2^+ of the ($B^2\Sigma$-$X^2\Sigma$) electronic system is shown also.

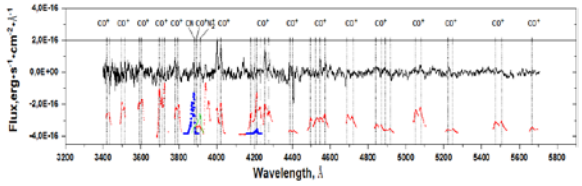

Figure 2: Linear spectrum and molecular emissions of the comet SW1. Color lines in bottom are the theoretical spectra predicted for the molecules *CN* (blue), N_2^+ (green) and CO^+ (red).

The N_2^+/CO^+ ratio is important in our understanding of the Solar System nebula formation. To estimate that ratio, we used integrated intensities of the CO^+ (2, 0) and N_2^+ 0, 0) bands. The column density (N) is defined by $N=L_{gv'v''}$, where L is the integrated band intensity and $gv'v''$ is the excitation factor. We used excitation factors of 7.0×10^{-2} photons·s^{-1}·mol^{-1} for the N_2^+ (0, 0) band and 3.55×10^{-3} photons·s^{-1}·mol^{-1} for the CO^+(2, 0) band. Finally, the ratio can be derived using the following expression:

$$\frac{N_2^+}{CO^+} = \frac{g_{CO^+}}{g_{N_2^+}} \cdot \frac{L_{N_2^+}}{L_{CO^+}}$$

If only the (2,0) band column density of CO^+ is used, then $[N_2^+] / [CO^+]$ should be equal to 0.01. The sublimation temperatures of *CO* and N_2 are 25 K and 22 K, respectively. Recent laboratory experiments indicate that the ice grains, which accumulated to produce the comet nuclei, were formed by freezing of water vapour at about 25 K. So, the comets may have been formed either beyond Neptune orbit, or at an early stage of the Solar System formation.

Summary and Conclusions

Using digital filters, we succeeded to isolate some structures in cometary coma (2 jets). Spectral dependence of the light scattering by the cometary dust obtained from the spectral observations of comet SW1 is typical for earlier observed comets: the mean value of the normalized spectral gradient equals to 11,31 ± 0,04% for the range 4430–5260 Å. SW1 is a CO^+ and $\boldsymbol{N_2^+}$ rich comet. The result suggests that the comets were possibly formed in a low temperature (about 25 K) environment. The value of $[\boldsymbol{N_2^+}]/[CO^+]$ is equal to 0.01.

Acknowledgements

This research is based on observations obtained at the Southern Astrophysical Research (SOAR) telescope, which is a joint project of the Ministério da Ciência, Tecnologia, e Inovação (MCTI) da República Federativa do Brasil, the U.S. National Optical Astronomy Observatory (NOAO), the University of North Carolina at Chapel Hill (UNC), and Michigan State University (MSU).

References

[1] Ivanova O.V, Luk'yanyk, I.V., Kiselev, N.N., et al. Photometry and spectral analyzing of activity the comet 29P/Schwassmann-Wachmann1, Planetary and Space Science, Vol. 121, pp.10–17, 2016

EPSC Abstracts
Vol. 11, EPSC2017-270-2, 2017
European Planetary Science Congress 2017

GR Precession and Kozai Mechanism in Asteroid-Comet Continuum

A. Sekhar (1,2), D. J. Asher (2), A. Morbidelli (3), S. C. Werner (1), J. Vaubaillon (4), G. Li (5)
(1) Centre for Earth Evolution and Dynamics, Faculty of Mathematics and Natural Sciences, University of Oslo, Norway (2) Armagh Observatory and Planetarium, Northern Ireland, United Kingdom, (3) Laboratoire Lagrange, Universite de Nice Sophia-Antipolis, CNRS, Observatoire de la Cote d'Azur, Nice, France (4) IMCCE Observatory of Paris, France (5) Harvard-Smithsonian Center for Astrophysics, Cambridge, MA, United States (aswin.sekhar@geo.uio.no)

Abstract

1. Introduction

Two well known phenomena associated with low perihelion distance bodies in orbital dynamics are general relativistic (GR) precession and Kozai oscillations.

The accurate prediction of the perihelion shift [17] of Mercury in accord with real observations is one of the signicant triumphs of the general theory of relativity [3]. Past works have looked into the GR precession in perihelion in different types of solar system bodies like planets, asteroids [14][13], comets [15][13] and meteoroid streams [4][12][5]. More recently some works have explored the cases of GR precession in exoplanetary systems [8].

In its purest form the Lidov-Kozai mechanism involves three bodies, namely a central body, test particle and perturber [7]. In real situations such as the solar system, the perturber is mainly Jupiter and the Kozai-like oscillations have a significant role in the orbital evolution [2][9] of many small bodies in the solar system.

In this work, we are interested to identify solar system bodies evolving in the near future (i.e. thousands of years in this case) into rapid sungrazing and sun colliding phases and undergoing inclination flips, due to Kozai-like oscillations and being GR active at the same time thus forming a GR-Kozai continuum phase space.

2. GR Precession and Kozai Mechanism Dynamics

We find that Kozai mechanism leads to secular lowering of perihelion distance which in turn leads to a huge increase in GR precession of the argument of pericentre depending on the initial orbital elements. This in turn gives feedback to the Kozai mechanism as the eccentricity, inclination and argument of pericentre in Kozai cycles are closely correlated. In this work, we find real examples of solar system bodies which show rapid enhancement in GR precession rates due to Kozai-like oscillations and there are cases where GR precession rate peaks to about 60 times that of the GR precession of Mercury thus showing the strength and complementary nature between these two dynamical phenomena. Comet 96P/Machholz 1 stands as a unique example in many of these aspects especially because its orbital connection [10][11] with two sungrazing comet families (Marsden and Kracht) and low perihelion distance meteoroid streams like Daytime Arietids and Southern Delta Aquariids . The orbital evolution of the body 322P/SOHO (can be considered as part of the asteroid-comet continuum) which was investigated in an interesting study[6] recently is also discussed.

An analytical treatment [9] is done on some solar system bodies to understand the difference in their orbital evolution in the context of Kozai mechanism with and without GR precession term by incorporating suitable Hamiltonian dynamics. Suitable conditions in phase space for sun colliding trajectories are found for cases evolving with and without GR precession to see the difference in the nature of their dynamical evolution. This result is subsequently matched using numerical integrations to find direct correlations for bodies which form the GR-Kozai continuum.

3. Summary and Discussion

Real solar system bodies showing both GR precession and Kozai-like oscillations are identified using compiled observational records from IAU-Minor Planet Center, Cometary Catalogue, IAU-Meteor Data Center by performing analytical plus numerical tests on them.

This intermediate state (where GR and Kozai effects

are comparable and co-exist forming a GR-Kozai continuum) brings up the interesting possibility of drastic changes in GR precession rates during orbital evolution due to sungrazing and sun colliding phases induced by the Kozai-like mechanism. Both these phenomena complementing and co-existing at the same time has interesting implications in the nodal geometry [1][16] and long term impact studies [18] on Earth from small bodies in general and the fate of small bodies ending up colliding with the sun.

Acknowledgements

Sekhar and Werner acknowledge the Crater Clock project (235058/F20) based at Centre for Earth Evolution and Dynamics (through the Centres of Excellence scheme project number 223272 (CEED) funded by the Research Council of Norway).

References

[1] Asher D. J., Steel D. I., 1996, MNRAS, 280, 1201.

[2] Bailey M.E., Chambers J.E., Hahn G., 1992, A&A, 257, 315.

[3] Einstein A. 1915, Preussische Akademie der Wissenschaften, Sitzungsberichte, 831.

[4] Fox K., Williams I.P., Hughes D.W. 1982, MNRAS, 199, 313.

[5] Galushina T. Yu., Ryabova G. O., Skripnichenko P. V., 2015, Planet. Space Sci., 118, 296.

[6] Knight M. M., Fitzsimmons A., Kelley M. S. P., Snodgrass C., 2016, ApJ, 823, L6.

[7] Kozai Y. 1962, AJ, 67, 591.

[8] Li G., Naoz S., Kocsis B., Loeb A., 2015, MNRAS, 451, 1341.

[9] Morbidelli A., 2011, Modern Celestial Mechanics: Aspects of Solar System Dynamics. Taylor & Francis/Cambridge Scientific Publishers.

[10] Ohtsuka K., Nakano S., Yoshikawa M., 2003, PASJ, 55, 321.

[11] Sekanina Z., Chodas P. W., 2005, ApJS, 161, 551.

[12] Sekhar A., 2013, WGN (J. Int. Meteor Organization), 41, 179.

[13] Sekhar A., Asher D. J., Werner S. C., Vaubaillon J., Li G., 2017, MNRAS, 468, 1405.

[14] Sitarski G., 1992, AJ, 104, 1226.

[15] Shahid-Saless B., Yeomans D.K., 1994, AJ, 107, 1885.

[16] Vaubaillon J., Lamy P., Jorda L., 2006, MNRAS, 370, 1841.

[17] Weinberg S. 1972, Gravitation and Cosmology: Principles and Applications of the General Theory of Relativity. Wiley, New York.

[18] Werner S. C., Ivanov B. A., 2015, in Schubert G., editor-in-chief, Treatise on Geophysics, 2nd edition, Vol. 10. Elsevier, Oxford, p. 327.

EPSC Abstracts
Vol. 11, EPSC2017-311-1, 2017
European Planetary Science Congress 2017

Prospects for studies of comets by the World Space Observatory Ultraviolet project

A. Kartashova, V. Sachkov and V. Emel'yanenko
Institute of Astronomy of the Russian Academy of Sciences, Moscow, Russia (akartashova@inasan.ru / Fax: +7-495-9515557)

Abstract

The World Space Observatory Ultraviolet (WSO-UV) [1], an international mission with Russia and Spain as the main contributors, consists of a 1.7m telescope with an imaging camera, two spectrographs in the range of 115-176 and 174-310 nm with a resolution of R = 50,000 for high resolution spectral observations and a long-slit-spectrograph for R=1,000 observations.

1. Introduction

The main scientific topics addressed by the project (included in the basic program) can be briefly summarized as follows:

- the baryon component of the Universe, the thermal and chemical evolution of the Universe;
- the formation and evolution of our Galaxy, the interaction of gas and stars, and the influence of magnetic fields on star formation;
- the physics of accretion and matter outflows;
- atmospheres of planets (exoplanets);
- the origin and physical evolution of comets.

The ultraviolet (UV) spectroscopy of comets at 110–320 nm wavelengths is a powerful tool of research, because this range of the electromagnetic spectrum contains the majority of resonance lines of atoms, molecules, and ions [2]. Due to the opacity of the Earth's atmosphere, such research can only be performed with space observatories. The World Space Observatory — Ultraviolet (WSO-UV) mission, planned for launch in 2023, will allow most of the challenges to be overcome in the UV studies of comets and will be able to become an essential research tool. Observations in the UV range are extremely necessary, because most astrophysical important resonant lines of atoms (O I, C I, H I, etc.), molecules (CO, CO_2, OH, etc.) and their ions lie in this range. In order to solve some of the problems, the UV data need to be complemented by ground-based observations.

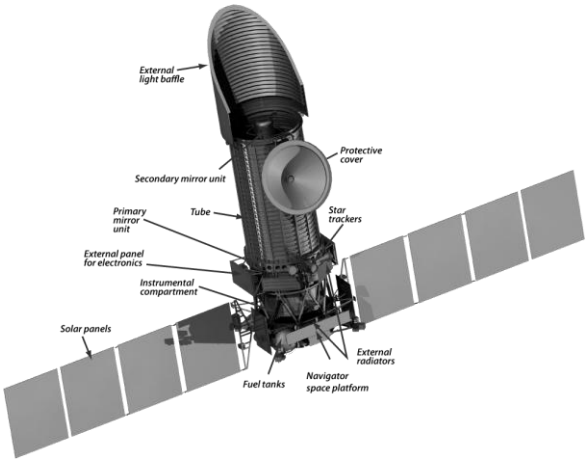

Figure 1: WSO-UV observatory model.

2. Conclusions

The information about the WSO-UV project is published at the website: *http://wso-uv.org*.

Acknowledgements

The work was partially supported by the RFBR grant № 16-02-00805-a, the RSF grant № 17-12-01441 and NSh - 9951.2016.2.

References

[1] Shustov B. M. et al.: WSO-UV progress and expectations, Ap&SS, Vol. 354, pp. 155 – 161, 2014.

[2] Sachkov M. E. et al.: Spectral Studies of Comets in the Ultraviolet Range and Prospects of the WSO-UV Project in these Studies, Solar System Research, Vol. 50, No. 4, pp. 294–299, 2016.

[3] Sachkov M.E.: UV observations of SDB stars and prospects of WSO-UV mission for such studies, Astrophys. Space Sci., Vol. 329, pp. 261–266, 2010.

EPSC Abstracts
Vol. 11, EPSC2017-318, 2017
European Planetary Science Congress 2017

Molecular oxygen formation from irradiation of ice grains in the protosolar nebula

O. Mousis (1), T. Ronnet (1), R. Maggiolo (2), A. Bouquet (3)
(1) Aix Marseille Université, CNRS, LAM (Laboratoire d'Astrophysique de Marseille) UMR 7326, 13388, Marseille, France (olivier.mousis@lam.fr), (2) Royal Belgian Institute for Space Aeronomy, BIRA-IASB, Ringlaan 3, B-1180 Brussels, Belgium, (3) Department of Space Science, Southwest Research Institute, 6220 Culebra Rd., San Antonio, TX 78228, USA

Abstract

Molecular oxygen has been detected in the coma of comet 67P/Churyumov–Gerasimenko with abundances in the 1–10% range by the Rosetta Orbiter Spectrometer for Ion and Neutral Analysis-Double Focusing Mass Spectrometer instrument (ROSINA) on board the Rosetta spacecraft. These observations suggest that O_2 was incorporated in the grains precursors of comets when they were in low-density environments such as the interstellar medium. Here, we investigate the possibility that O_2 was produced in the protosolar nebula when cometary grains were lifted toward its upper layers and dragged down over a large number of cycles, due to turbulent mixing.

1. Introduction

Molecular oxygen has been detected in the coma of comet 67P/Churyumov–Gerasimenko (67P/C-G) with abundances in the 1–10% range by the Rosetta Orbiter Spectrometer for Ion and Neutral Analysis-Double Focusing Mass Spectrometer instrument on board the Rosetta spacecraft [1]. To account for this observation, it has been recently shown that the radiolysis of icy grains is not fast enough in the protosolar nebula (PSN) to create sufficient amounts of O_2 over its lifetime [2]. It has been then proposed that 67P/C-G agglomerated from icy grains originating from ISM instead of condensing in the protosolar nebula because low-density environments such as molecular clouds allow the radiolysis to work in an efficient manner [2]. Here, we investigate the alternative possibility that the icy grains condensed in the protosolar nebula midplane before their agglomeration by comets. Due to turbulent mixing, these grains were lifted toward the upper layers of the disk and dragged them down over a large number of cycles [3]. In our model, these grains spend a non-negligible fraction of their lifetime in the disk's upper regions, where the irradiation is strong.

2. Model

To mimic the vertical motion of particles, we used a simple description of the PSN structure [4, 5] and the transport module of particles described in [6]. Our calculations have been performed at a distance of 30 AU from the Sun. Once the trajectories of particles have been determined, we used the approach of [7] to compute the energy rate received from cosmic rays irradiation by water molecules as a function of the column density of the gas.

3. Results

As illustrated by Figure 1, turbulence plays an important role in the motion of small dust grains that are well coupled to the gas. Micron-sized grains initially settled in the midplane are entrained by turbulent eddies and diffuse radially and vertically with an effective viscosity roughly equal to that of the gas for such small particles [5]. Consequently, solid particles follow a Gaussian distribution in the vertical direction. The scale height of dust (corresponding to the standard deviation of the distribution) is a fraction of the gas scale height, this fraction being larger and possibly equal to the gas scale height in the cases of small grains and higher degrees of turbulence. Figure 2 represents the vertical distribution of 1 cm particles computed with our transport/disk model, assuming a coefficient of turbulent viscosity $\alpha = 10^{-3}$. Figure 3 shows the evolution of the O_2/H_2O ratio in 1 cm particles as a function of time. The resulting abundance of oxygen is at best four orders of magnitude lower than the one observed by the Rosetta spacecraft.

4. Discussion

Our preliminary computations suggest that, even if a significant fraction of the icy particles has been lifted toward the upper layers of the disk over several hun-

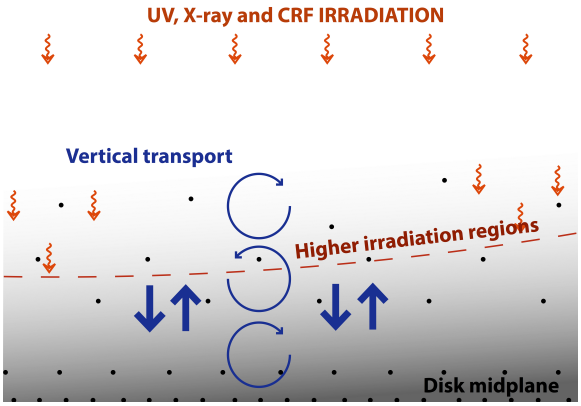

Figure 1: Illustration of the vertical transport of small icy grains toward disk regions where they are efficiently irradiated (see [3]). Dust is concentrated in the midplane of the disk due to gravitational settling and gas drag. However, turbulent eddies lift the icy grains toward the upper regions and also drag them down because the direction of the velocity is random and consistent during a timescale comparable to the local keplerian period.

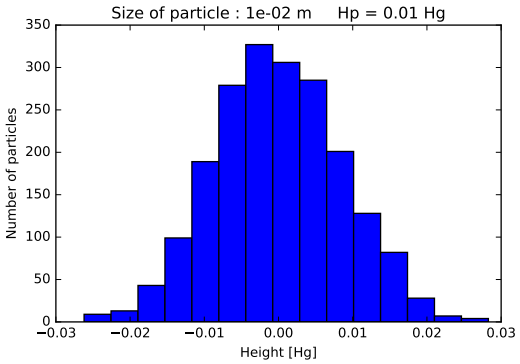

Figure 2: Vertical distribution of 10^{-2} m particles at 30 AU in the PSN.

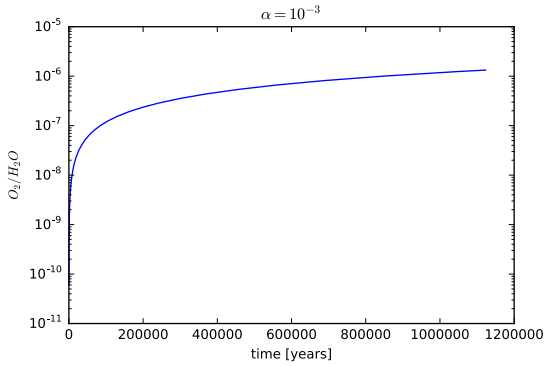

Figure 3: Abundance of O_2 relative to H_2O in 1 cm particles as a function of time. The O_2 abundance reaches a plateau at $\sim$0.8 Myr.

dred thousands years during the PSN evolution, the amount of O_2 created via radiolysis cannot account for the Rosetta observations. However, only simulations of the vertical transport of 10^{-2} m particles with a unique α value have been investigated. To provide a more robust conclusion, we need to investigate the full domain of plausible α values as well as different sizes of particles in the 10^{-6}–10^{-2} m range.

References

[1] Bieler, A., and 32 colleagues 2015. Abundant molecular oxygen in the coma of comet 67P/Churyumov-Gerasimenko. Nature 526, 678-681.

[2] Mousis, O., and 7 colleagues 2017. Stability of Sulphur Dimers (S_2) in Cometary Ices. The Astrophysical Journal 835, 134.

[3] Mousis, O., and 15 colleagues 2016. Origin of Molecular Oxygen in Comet 67P/Churyumov-Gerasimenko. The Astrophysical Journal 823, L41.

[4] Chiang, E. I., Goldreich, P. 1997. Spectral Energy Distributions of T Tauri Stars with Passive Circumstellar Disks. The Astrophysical Journal 490, 368-376.

[5] Ciesla, F. J., Sandford, S. A. 2012. Organic Synthesis via Irradiation and Warming of Ice Grains in the Solar Nebula. Science 336, 452.

[6] Ronnet, T., Mousis, O., and Vernazza, P. Pebble Accretion at the Origin of Water in Europa. The Astrophysical Journal, submitted

[7] Yeghikyan, A. G. 2011. On the Cosmic Ray-Induced Ionization Rate in Molecular Clouds. ISRN Astronomy and Astrophysics 2011, 905015.

EPSC Abstracts
Vol. 11, EPSC2017-343-1, 2017
European Planetary Science Congress 2017

Towards a unique formation and trapping scenario of O_2 and S_2 in comets

F. Pauzat (1), O. Ozgurel (1), Y. Ellinger (1), A. Markovits (1) and O. Mousis (2)
(1) Sorbonne Universités, UPMC Univ Paris 06, CNRS UMR 7616, LCT, F-75252 Paris, France,
(2) Aix Marseille Univ, CNRS, LAM, UMR 7326, F-13388 Marseille, France
(pauzat@lct.jussieu.fr)

Abstract

Following the observations by the ROSINA-DFMS instrument on board of Rosetta spacecraft, the processes of formation of O_2 and S_2 in comets are actually quite disputed and a consistent interpretation of all the data is still to be found. Computational chemistry models based on first principle periodic density functional theory (DFT) are well adapted to the description of compact ice and are shown here to be capable to provide the quantitative data to support the following scenario for O_2 and S_2 origin in 67P. In this scenario, assuming that both, O_2 and S_2, should have similar ways of formation, storage and release, we propose that these dimers were formed inside the icy grains precursors of comets in low-density environments by irradiation, photolysis and/or radiolysis, which creates simultaneously voids in the compact ices, voids within which the molecules produced can be trapped efficiently enough to be liberated only simultaneously with the water ices.

1. Observational background

The search for O_2 in space has been carried on for years to no avail, even if now some old observations are re-considered as positive; on the contrary, S_2 has been observed for decades in comets. Nevertheless, both molecules suddenly arose a new interest following their observation in comet 67P/Churyumov-Gerasimenko (67P/C-G) [1] [3]. The ROSINA-DFMS instrument on board of the Rosetta spacecraft detected molecular oxygen in the coma with an unexpected range of abundances (1–10% with respect to H_2O) and a surprising correlation with H_2O. Concerning S_2, the abundance observed is much lower though significant (~10^{-5} with respect to H_2O) but shows no correlation with H_2O [2].

2. One formation scenario

We propose that both molecules, O_2 and S_2, are formed in the icy grain precursors of comets by irradiation (photolysis and/or radiolysis) respectively of the H_2O ices themselves, or of the S-bearing molecules embedded in the H_2O ices. The cosmic ray flux simultaneously creates voids in the matrix within which the so produced molecules can accumulate.
For both molecules, such a formation inside the grains must occur in low-density environments such as the ISM or the upper layers of the protosolar nebula, where the local temperature is extremely low. In the first case, comets would have agglomerated from icy grains that remained pristine when entering the nebula. In the second case, comets would have agglomerated from icy grains condensed in the protosolar nebula and that would have been efficiently irradiated during their turbulent transport toward the upper layers of the disk.

2.1 The case of O_2

In this scenario, the irradiation is assumed to break the H_2O molecules along their tracks, inducing a chemistry of highly reactive radicals as H, O, OH, leading in particular to the formation of O_2. The voids created simultaneously in the compact ices home the molecules produced and keep them trapped efficiently enough to get them liberated only when the water ices sublimate, even if a moderate heating eventually occurs, allowing an amorphous-to-crystalline phase transition.

Indeed, we have studied the stability of the O_2 molecules in different types of cavities (Table 1), and got the following results: i) no stabilization can be found neither for the inclusion of O_2 in the hexagonal ice lattice, nor for the replacement of a H_2O by O_2, ii) by contrast, the irradiation of the ice by cosmic rays generates cavities in which molecular oxygen is

perfectly stable under the form of O_2 or even of dimers of O_2, a possibility which allows to interpret the variations of the proportion O_2/H_2O observed [4].

Table 1: Stability (eV) of O_2 in voids within the ice (n: number of molecules removed to create the void)

Environment	H_2O ices
Inclusion (n=1)	0.00
Inclusion (n=2)	0.23
Inclusion (n=4)	0.25
Inclusion (fine track)	0.24
Inclusion (large track)	0.30

2.2 The case of S_2

It is well known chemically that S-bearing molecules embedded in H_2O ices turn easily to SH_2 under irradiation effects, making possible the creation of sort of clumps within the H_2O lattice; knowing that, under more irradiation, the SH_2 molecules convert themselves into S_2 and even larger oligomers, we considered again the possibility that these molecules can accumulate in the voids created simultaneously in the icy matrix.
We have investigated the stability of the S_2 molecules in such cavities, assuming that the surrounding ice could be made of H_2S or H_2O (Table 2). We show that the stabilization energy of S_2 molecules in such voids is close to that of the H_2O ice binding energy, implying that they can only leave the icy matrix when this latter sublimates.

Table 2: Stability (eV) of S_2 in voids within the ice (n: number of molecules removed to create the void)

Environment	H_2O ices	H_2S ices
Inclusion (n=1)	Non stable	0.30
Inclusion (n=2)	0.30	0.40
Inclusion (n=4)	0.50	0.40
Inclusion (fine track)	0.51	0.41
Inclusion (large track)	0.53	0.50

However, as S_2 can be trapped in H_2O as well as in SH_2 environments, no correlation has to be found with H_2O emission [5].

3. Summary and Conclusions

Both molecules O_2 and S_2 detected in the coma of 67P/C-G might have been formed inside the icy grains precursors of comets in low-density environments as a consequence of the cosmic rays irradiation. Using computational chemistry models based on first principle periodic density functional theory (DFT), we have evaluated the stability of these species in the irregular cavities of the irradiated compact ices, revealing a strong stabilization, efficient enough to keep them trapped until the ices sublimate.

The high abundance observed for O_2 can be explained by the quasi-unlimited raw material available, H_2O. It should be stressed that the formation of one O_2/S_2 requires at least the destruction of two H_2O /SH_2 whatever the chemical reactions involved. Consequently, O_2 formed and trapped only in an H_2O environment should be correlated strongly to the H_2O emission, contrary to S_2 possibly formed and trapped in different matrices.

Specific calculations on the chemistry of formation of the two species inside the icy bulk are actually in progress.

References

[1] Bieler, A., Altwegg, K., Balsiger, H., et al., Abundant molecular oxygen in the coma of comet 67P/ Churyumov-Gerasimenko, Nature, 526, 678, 2015.

[2] Calmonte U., Altwegg K., Balsiger H., et al, Sulfur-bearing species in the coma of comet 67P/Churyumov-Gerasimenko, MNRAS, 462, S253, 2016.

[3] Le Roy, L., Altwegg, K., Balsiger, H., et al., Inventory of the volatiles on comet 67P/Churyumov-Gerasimenko from Rosetta/ROSINA, A&A, 583, A1, 2015.

[4] Mousis O., Ronnet, Brugger B., Ozgurel O et al., Origin of molecular oxygen in Comet 67P/Churyumov-Gerasimenko, ApJL, 823, L41, 2016.

[5] Mousis O., Ozgurel O., Lunine J.I. et al, Stability of sulphur dimers (S_2) in cometary ices, A&A, 835 :134, 2017.

EPSC Abstracts
Vol. 11, EPSC2017-442, 2017
European Planetary Science Congress 2017

The active binary asteroid 288P (300163)

J. Agarwal[1], D. Jewitt[2,3], M. Mutchler[4], H. Weaver[5], S. Larson[6]
(1) Max-Planck-Institut für Sonnensystemforschung, Göttingen, Germany (agarwal@mps.mpg.de), (2) Department of Earth, Planetary and Space Sciences, University of California at Los Angeles, USA (3) Department of Physics and Astronomy, University of California at Los Angeles, USA, (4) Space Telescope Science Institute, Baltimore, USA, (5) The Johns Hopkins University Applied Physics Laboratory, Laurel, USA, (6) Lunar and Planetary Laboratory, University of Arizona, USA.

Abstract

We report on Hubble Space Telescope observations of the active asteroid 288P (300163) that reveal it to be a binary system, and confirm sublimation as the most likely cause of the activity. The observations were obtained at 12 epochs between August 2016 and January 2017, covering both the perihelion and a close perigee of 288P. The combination of similarly sized components, a wide separation, high eccentricity, and activity renders 288P unique among the known binary asteroids. We discuss rotational fission and an impact as possible formation scenarios, and explore the influence of the activity on the evolution of the system.

EPSC Abstracts
Vol. 11, EPSC2017-482, 2017
European Planetary Science Congress 2017

Layerings in cometary nuclei

B.-K. Ruzicka (1,2, ruzicka@mps.mpg.de), H. Böhnhardt (1), A. Pack (2)
(1) Max Planck Institute for Solar System Research, Göttingen, Germany
(2) University of Göttingen, Germany

Comets are believed to have been formed in the outer regions of the solar nebula, and may thus allow us to constrain the chemical, mineralogical, and physical conditions in the early solar system. Several cometary nuclei visited by spacecraft appear to have a surface that consists of layered material. These layerings help us understand whether the nuclei formed as rubble piles by hierarchical accretion, or through streaming instabilities, or if a hybrid model is most appropriate [1]. Their curvature and orientation also indicate whether comets are primordial bodies or collisional remnants of much larger bodies.

When the Rosetta spacecraft arrived at comet 67P/Churyumov-Gerasimenko, its instruments returned data of unprecedented scope and resolution, which made possible a detailed examination of the layerings on the nuclei of a comet. An initial study of these layerings found that the comet appears to consist of two independent lobes that are concentrically layered to a depth of several hundred meters below the surface [2].

In order to take measurements of three-dimensional structures on the surface of cometary nuclei, we project images onto a shape model of the nucleus. In the case of comet 67P we used data from the OSIRIS Narrow Angle Camera and a shape model produced from these images. We extrapolate the orientation of potential layerings by mapping discontinuity surfaces where they are exposed at cliffs and hillsides (Figure 1), and by projecting them into the nucleus surface. We model the global orientation of the layerings by fitting ellipsoidic shells to our measurements [3].

Results of the measurements and analysis of the layerings are presented and compared to findings by Penasa et al. [3].

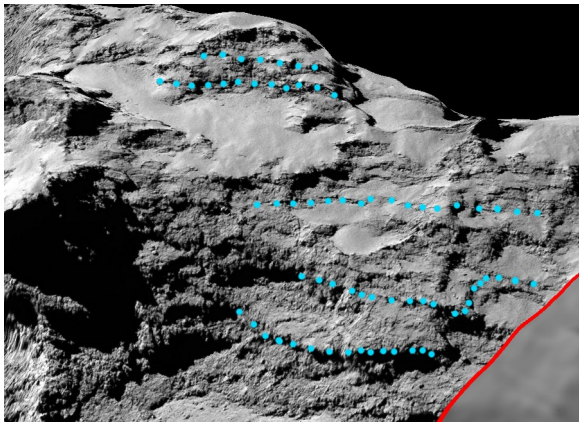

Figure 1: Screenshot of the software used for mapping, which projects OSIRIS images (framed in red) onto a shape mode (visible in lower right corner). Blue dots represent locations of measurements.

Acknowledgements

We use software provided by CNES and Magellium. Our work is benefiting greatly from the constructive collaboration with Dr. Massironi and Dr. Penasa. A subset of OSIRIS data was provided by Dr. Sierks.

References

[1] Davidsson, B., Sierks, H., Güttler, C., et al..: The primordial nucleus of comet 67P/Churyumov-Gerasimenko, Astronomy & Astrophysics, Vol. 592, A63, 2016.

[2] Massironi, M., Simioni, E., Marzari, F., et al.: Two independent and primitive envelopes of the bilobate nucleus of comet 67P, Nature, Vol. 526, P. 402-405, 2015.

[3] Penasa, L., Massironi, M., Naletto, G., et al.: A three dimensional modelling of the layered structure of comet 67P/Churyumov-Gerasimenko, Monthly Notices of the Royal Astronomical Society, submitted.

EPSC Abstracts
Vol. 11, EPSC2017-537-1, 2017
European Planetary Science Congress 2017

Spectral properties of near-Earth asteroids on cometary orbits

M. Popescu (1,2), O. Vaduvescu (3,4,5), J. de León (3,4), I. L. Boaca (1), R.M. Gherase(1), D.A. Nedelcu (1,2) and ING/INT students (5)
(1) Astronomical Institute of the Romanian Academy, 5 Cuţitul de Argint, 040557 Bucharest, Romania, *mpopescu@imcce.fr*; (2) IMCCE, Observatoire de Paris, PSL Research University, CNRS, Sorbonne Universités, UPMC Univ Paris 06, Univ. Lille, France; (3) Instituto de Astrofísica de Canarias (IAC), C/Vía Láctea s/n, 38205 La Laguna, Tenerife, Spain; (4) Departamento de Astrofísica, Universidad de La Laguna, 38206 La Laguna, Tenerife, Spain; (5) Isaac Newton Group of Telescopes (ING), Apartado de Correos 321, E-38700 Santa Cruz de la Palma, Canary Islands, Spain.

Abstract

A fraction of near-Earth asteroids has orbital characteristics similar to comets. In a first approximation based on dynamical models, the near-Earth asteroids on cometary orbits (NEACOs) can be defined as NEAs with Jovian Tisserand parameter $T_J < 3$. Up to now (April 21, 2017), about 956 objects (6%) out of 16030 NEAs are in this category.

We aim to study the spectral distributions of NEACOs and to identify those with cometary origin. We present the spectral observations for 19 NEACOs consisting of 16 visible spectra obtained with the 2.5m Isaac Newton Telescope and 9 near-infrared (NIR) spectra obtained with the NASA Infrared Telescope Facility (IRTF). Although initially classified as asteroid, one of our targets - 2007 VA85 was confirmed to be active comet 333P/LINEAR on its 2016 appearance.

To complement our dataset we retrieved taxonomic classification for another 57 objects from EARN - DLR database. Therefore, we studied the taxonomic distribution of 76 asteroids, out of which 49 are numbered asteroids. This sample represents about 8 $\%$ of the known NEACOS and it is four time larger compared to previous works [1, 2].

We found that the NEACOs population is a mixing of different spectral types and their taxonomic distribution varies significantly with the value of T_J. The Q,S-complex,taxonomical types associated to olivine-pyroxene compositions are about $\sim 70\%$ for the objects satisfying $2.9 < T_J < 3$ in our sample, while the objects classified as B,C,X and D types - which can be associated with cometary nuclei, are dominant (21 out of 29 objects) for $T_J < 2.7$. A particular interesting case is that of (466130) 2012 FZ23 which has a $T_J = 2.367$ and exhibits a R/Sr type spectrum.

1. Introduction

Asteroids and comets have been considered as a two distinct types of objects. They formed at different distances of the young Sun, thus, their composition is characteristic of the region where they formed. The first distinction is that the comet nuclei are surrounded by a coma produced by the outgasing of volatiles when approaching the Sun. The discovery of extinct or dormant comets which show asteroidal appearance as well as the asteroid outburst required to review the definition of these objects (e.g. [3]).

In most of the cases, the cometary orbits have $T_J < 3$, while the majority of asteroids have $T_J > 3$. From physical point of view, the active, dormant and dead comets are very dark, often reddish, objects , with spectra similar to D, P, and C-type asteroids and with albedos and color probably controlled by carbonaceous dust containing reddish organic compounds (e.g. [4]). Their spectra describe objects that are the most pristine observable Solar System objects.

In this work we discuss the spectral properties of 76 NEACOs. We show new visible and NIR spectra for 19 objects observed with the INT and with the IRTF telescopes. Our set was complemented with another 57 objects classified taxonomically in order to derive a taxonomical distribution relative to T_J parameter.

2. Spectral data

We obtained new spectra of 19 NEACOs using the 2.54 m INT (16 observations), and the 3m IRTF (9 observations) telescopes. For two objects we joined our visible part with near-infrared information available at MIT-UH-IRTF database.

We used the IDS longslit spectrograph (INT) with the R150V diffraction element and the RED2+ camera in order to cover the spectral interval 0.4-0.92 μm. We used the SpeX instrument, with the 0.8x15" slit, in the low resolution mode to obtain spectra over 0.8-2.5 μm interval.

We classified each spectrum in the Bus-DeMeo taxonomic system by using the MIT-SMASS on-line tool (for vnir spectra) and by performing curve matching with the 25 classes defined by this taxonomy (using M4AST website). The results are summarized in Table 1.

Table 1: The asteroids observed with the INT and the IRTF telescope. The '*' shows data from MIT-UH-IRTF database.

Desig.	Tj	Taxon.	Spec. interval
2007 VA85	0.418	D	nir
466130	2.367	R/Sr	nir
248590	2.441	T/D	nir
433992	2.566	D	vis+nir
414287	2.619	Xk/B	vis+nir*
450160	2.689	S	nir
413192	2.779	X	vis
1998 GL10	2.788	X	vis
442037	2.816	Cg/K	vis+nir*
2015 XB379	2.82	L	vis+nir
214088	2.845	Sq	vis+nir
2015 WH9	2.88	Xk	vis
430439	2.929	T /D	vis
9400	2.94	Sq	vis
293054	2.945	S	vis
2015 CA1	2.96	T	vis
2011 YB40	2.985	Q	vis
416071	2.993	Sr	vis+nir
417264	2.997	Xc	vis+nir

3. Results

We complemented our sample using data existing in the EARN-DLR database. We searched for asteroids unambiguously classified and found information for other 56 NEACOs. Therefore, the total data set includes 76 objects which include 49 numbered asteroids. Except 2007 VA85 ($T_J = 0.418$) which was confirmed as an active comet, all of them have orbits similar to Jupiter Family Comets ($2 < T_J < 3$).

For a statistical analysis we divided the data in two groups: Q/S group (silicate-like) - objects classified as Q or S-complex and which are associated with olivine-pyroxene compositions, and B/C/X/D group (cometary-like) - objects classified as B,C,X,T and D types - which are featureless spectra and may represent a carbonaceous chondrite composition and organic compounds, similar to a cometary nuclei. We note that X class represents three distinct types (E - enstatite, M-metallic, and P-primitive) which can be differentiated by their albedo and only the P class may represent an extinct or dormant comet.

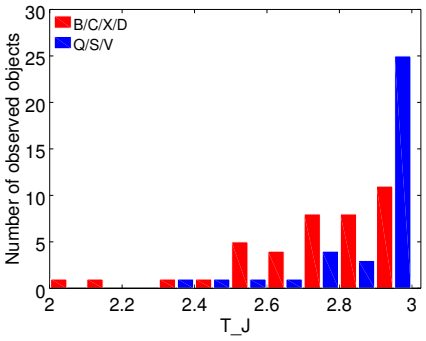

Figure 1: The taxonomic distribution relative to the T_J parameter. A 0.1 width bin on Ox axe was used.

The histogram plotted in Fig.1 shows that the ratio of silicate-like versus cometary-like objects varies significantly with the value of T_J. The Q,S-complex taxonomical types are about $\sim 70\%$ (25 out of 36) for the objects satisfying $2.9 < T_J < 3$ in our sample. The objects classified as B,C,X and D types represent the majority - 21 out of 29 objects, for $T_J < 2.7$. Although subject to different biases (including observational and discovery biases), this distribution shows that there is no strict correlation between the T_J factor and the object composition. Two particular cases within this distribution are those of (466130) 2012 FZ23 which has a $T_J = 2.367$ and exhibits a spectrum similar to R/Sr type and of (455426) 2003 MT9, $T_J = 2.591$ which has an S/Sr spectrum.

Although on its discovery 2007 VA85 was classified as asteroid, on its close approach from 2016 a cometary activity was detected, thus receiving the designation 333P/LINEAR. The observation performed with IRTF/SPEX on March 09, 2016 shows a very red spectrum compatible with a D-type object [5].

Acknowledgements

This research use the data provided by E.A.R.N. - The Near-Earth Asteroids Data Base ($http://earn.dlr.de/nea/$), MIT-UH-IRTF Joint Campaign for NEO Reconnaissance ($http://smass.mit.edu/$) and JPL Small-Body Database Browser ($https://ssd.jpl.nasa.gov/sbdb.cgi$). We thank to INT/ING students R. Ashley, M. Diaz Alfaro, R. Errmann, F. Lopez, I. Ordonez, H.F. Stevance for their support with INT/IDS observations. The work of M. Popescu, I. L. Boaca, R.M. Gherase and D.A. Nedelcu was supported by a grant of the Romanian National Authority for Scientific Research – UEFISCDI, project number PN-II-RU-TE-2014-4-2199.

References

[1] Licandro, J., Alvarez-Candal, A., de León, J., et al. (2008), Astronomy and Astrophysics, 481, 861

[2] DeMeo, F. & Binzel, R. P. (2008), Icarus, 194, 436

[3] Tancredi, G. (2014), Icarus, 234, 66

[4] Hartmann, W. K., Tholen, D. J., & Cruikshank, D. P. 1987, Icarus, 69, 33

[5] Licandro, J., et al, (2017) paper in preparation

EPSC Abstracts
Vol. 11, EPSC2017-569, 2017
European Planetary Science Congress 2017

Evidence for low tensile strength in comet nuclei

R. Kokotanekova (1,2), C. Snodgrass (2), P. Lacerda (3), S. C. Lowry (4), Y. R. Fernández (5), S. F. Green (2), C. Tubiana (1), A. Fitzsimmons (3) and H. H. Hsieh (6,7)
(1) Max Planck Institute for Solar System Research, Germany, (2) The Open University, UK, (3) Queen's University Belfast, UK, (4) The University of Kent, UK, (5) University of Central Florida, USA, (6) Planetary Science Institute, USA, (7) Institute of Astronomy and Astrophysics, Academia Sinica, Taiwan (kokotanekova@mps.mpg.de)

Abstract

We provide an updated study of the collective properties of Jupiter Family comets (JFCs) by increasing the sample of comets with well-studied rotation periods and surface characteristics. To collect the sample, we review the properties of 35 JFCs with published rotation rates and add new lightcurves and phase functions for nine JFCs observed between 2004 and 2015. We use the extended sample of 37 comets to characterise the bulk density, tensile strength, collisional history and surface properties of JFCs. Using the model for stability of rotating solid biaxial ellipsoids [1], we conclude that none of the observed JFCs require tensile strength larger than 10-25 Pa to remain stable against rotational breakup.

1. Introduction

Time-series photometric observations of comet nuclei can be used to derive the comets' lightcurves and phase functions. Lightcurves are a rich source of information on the spin and shape properties of comets, and can be used to constrain the collisional history, density and strength of JFCs. Deriving the phase functions and albedos of the nuclei allows us to study the surface properties of JFCs and to compare them to other small-body populations in the Solar system.

The collective properties of JFCs were reviewed over a decade ago [3, 5]. In this work, we update the sample of JFCs with known rotation properties with the results published since the last review [5] and add our newly obtained results on nine comets.

The newly analysed comets were observed with a number of ground-based telescopes as part of the Survey of Ensemble Physical Properties of Cometary Nuclei (SEPPCoN, [2]) as well as during devoted phase function observing campaigns. In order to combine the different datasets we developed a method for absolute photometric calibration using stars from the Pan-STARRS survey. This approach allowed us to combine data sets taken at different epochs and instruments with photometric precision down to 0.03 mag.

2. Results and Conclusions

We review the properties of 35 JFCs with previously studied rotation rates and present the analysis of ground photometric observations of nine comets. The total number of comets in the updated sample is 37. The main results of this work are as follows:

- We improve the rotation periods for comets 14P/Wolf, 47P/Ashbrook-Jackson, 94P/Russell, and 110P/Hartley 3 and determine the rotation rates of comets 93P/Lovas and 162P/Siding-Spring for the first time.
- We determine the phase functions for seven of the examined comets and derive albedos for eight of them.
- The new extended sample confirms the known cut-off in bulk density at ~ 0.6 g cm^{-3} [3] assuming that JFCs are strengthless bodies.
- Assuming the model of [1] for prolate ellipsoids with typical density and elongations, we determine that JFCs require tensile strength not larger than 10-25 Pa to remain stable against rotational instabilities (Fig. 1).
- Using the newly derived albedos and phase functions, we determine that the median linear phase function coefficient for JFCs is 0.046 mag/deg and the median albedo is 4.2 per cent.
- We find evidence for an increasing linear phase function coefficient with increasing albedo (Fig. 2).

These findings allow us to compare JFCs to other populations in the Solar System in a search for evidence for JFC origins.

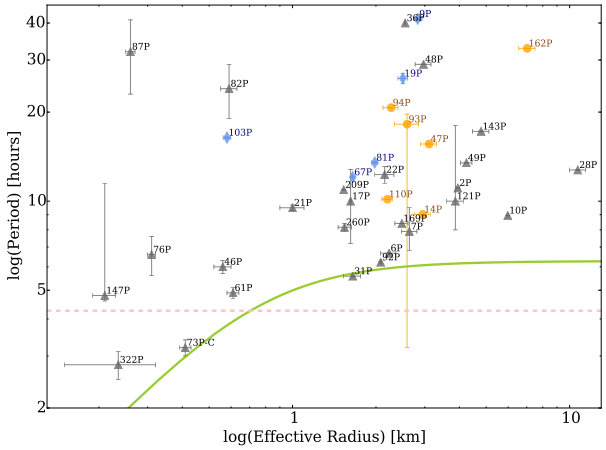

Figure 1: Rotation period against effective radius of the JFC nuclei. The blue diamonds correspond to comets visited by spacecraft; the grey triangles are comets observed from ground and the orange circles are the JFCs added in this work. The dashed pink line shows the minimum possible rotation rate for strengthless spherical bodies with density $\rho = 0.6$ g cm^{-3}. The green curve is derived from the model for prolate ellipsoids stable against rotational instability [1]. The curve shows the model for density $\rho = 532$ kg m^{-3}, axial ratio $a/b = 2$ and tensile strength $T = 15$ Pa, which corresponds to the parameters measured for 67P from Rosetta. We can conclude that for typical densities and axial ratios, the observed comets do not require tensile strength larger than 10-25 Pa in order to remain stable against rotational splitting.

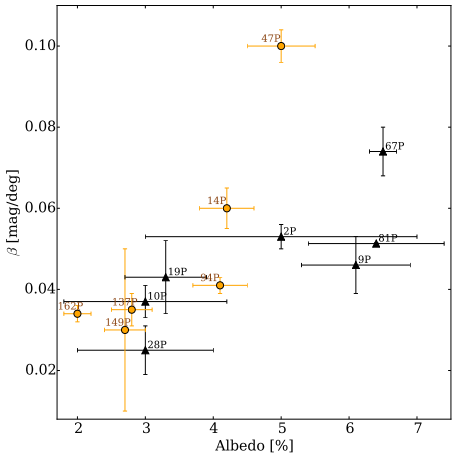

Figure 2: Phase function slope versus albedo of all JFCs with known radius, albedo and phase function. The orange circles correspond to comets with properties derived in this work. There is an indication for a trend of increasing phase function slope with increasing albedo.

References

[1] Davidsson, B. J. R.: Tidal splitting and rotational breakup of solid biaxial ellipsoids, Icarus, Vol. 149, pp. 375–383, 2001.

[2] Fernández, Y. R., Kelley, M. S., Lamy, P. L., Toth I. et al.: Thermal properties, sizes, and size distribution of Jupiter-family cometary nuclei, Icarus, Vol. 226, pp. 1138–1170, 2013.

[3] Lamy, P. L., Toth, I., Fernandez, Y. R. and Weaver, H. A.: The sizes, shapes, albedos, and colors of cometary nuclei, Comets II, University of Arizona Press, pp. 223-264, 2004.

[4] Lowry, S. C. and Weissman, P. R.: CCD observations of distant comets from Palomar and Steward Observatories, Icarus, Vol. 164, pp. 492–503, 2003.

[5] Snodgrass, C., Lowry, S. C. and Fitzsimmons, A.: Photometry of cometary nuclei: rotation rates, colours and a comparison with Kuiper Belt Objects, Monthly Notices of the Royal Astronomical Society, Vol. 373, pp. 1590–1602, 2006.

EPSC Abstracts
Vol. 11, EPSC2017-582-1, 2017
European Planetary Science Congress 2017

Inactive Comets from the Oort Cloud: Manxes are Tracing the History of Solar System Formation

O. R. Hainaut[1], K. J. Meech[2], B.Yang[3], S. Berdyugina[4], J. V. Keane[2], M. Micheli[5,6], A. Morbidelli[7], R. J. Wainscoat[2]

1: European Southern Observatory, Garching, Germany – 2: Institute for Astronomy, Honolulu, HI, USA – 3: European Southern Observatory, Santiago, Chile – 4: Kiepenheuer Institut fuer Sonnenphysik, Freiburg, Germany – 5: ESA SSA-NEO Coordination Centre, Frascati (RM), Italy – 6: INAF - Osservatorio Astronomico di Roma, Monte Porzio Catone (RM), Italy – 7: Obs. de la Cote d'Azur, Nice, France

Abstract

Manx comets are nearly tailless objects on long-period comet (LPC) orbits, in strong contrast to the appearance of normal LPCs. They may early inner solar system remnants, ejected to the Oort cloud at the time of planet formation. The fraction of rocky objects on these orbits sets strong constraints on the dynamical models attempting to reproduce our current solar system. We present our program to observe Manx comets and the implications on the early solar system.

1. Introduction

Recent dynamical models succeed in reproducing key characteristics of our current solar system [1]; some of these models require significant migration of the giant planets, while others do not. These models provide very different predictions on the presence of rocky inner solar system material expelled from the inner Solar System into the Oort cloud.

Determining the amount of S-type material present in the Oort cloud could therefore be the key to verifying the predictions of the planet migration-based dynamical models.

The Pan-STARRS1 telescope is now the most prolific facility discovering inactive and very low activity comets on long-period comet orbits, the Manx comets. As they are now numerous enough for a population study, and thanks to the availability of large telescopes allowing us to characterize them, we embarked on a program to study the surface of Manx comets, in order to identify the rocky ones and to estimate their fraction.

2. Observations

A detailed statistical analysis indicated that measurements of a sample of 50 Manx comets will allow us to rule out some of the dynamical models representing the early solar system, depending on the number of S-type Manx objects present in the sample. The size of the sample is a good trade-off between the amount of observation time required and the constraints on our current (lack of) knowledge on the early times of the solar system.

We secured time on the ESO Very Large Telescope (VLT) and Gemini North (GN) to acquire visible and near-IR photometric observations.

Our current list of Manx candidates includes 87 objects. While 31 of these were lost or became too faint before we could schedule observations, we already secured spectrophotometric observations on 22 objects, and 5 more are queued on GN and 6 on the VLT.

One of these Manx objects, C/2014 S3 (PANSTARRS), has a surface that is physically similar to an inner main belt rocky S-type asteroid (see Fig.1 for a spectrum and [1] for details). Modern inner solar system S-type asteroids are rocky and do not possess volatiles [2]. However C/2014 S3 displays a very faint, weak level of comet-like activity. The activity implies that C/2014 S3 has retained a tiny fraction of the water that is expected to be present at its formation distance in the inner solar system [3]. We may be looking at fresh inner solar system Earth-forming material that was ejected

from the inner solar system and preserved for billions of years in the Oort cloud.

Our survey of Manx comets is now about half-way to the required sample of 50 objects. At this stage, one S-type object was identified, and the others present a wide variety of colours, from neutral to very red, a much greater diversity of surfaces than that of comet surfaces.

This presentation will report on the current status of our survey and possibly propose some first conclusions on the consequences on the early solar system

Fig.1: Reflectivity spectrum for Manx comet C/2014 S3, from the CFHT in Oct.2014 andVLT in Nov.2014, and spectra of six S-type asteroids. All spectra are normalized to 1 at 0.65 mm

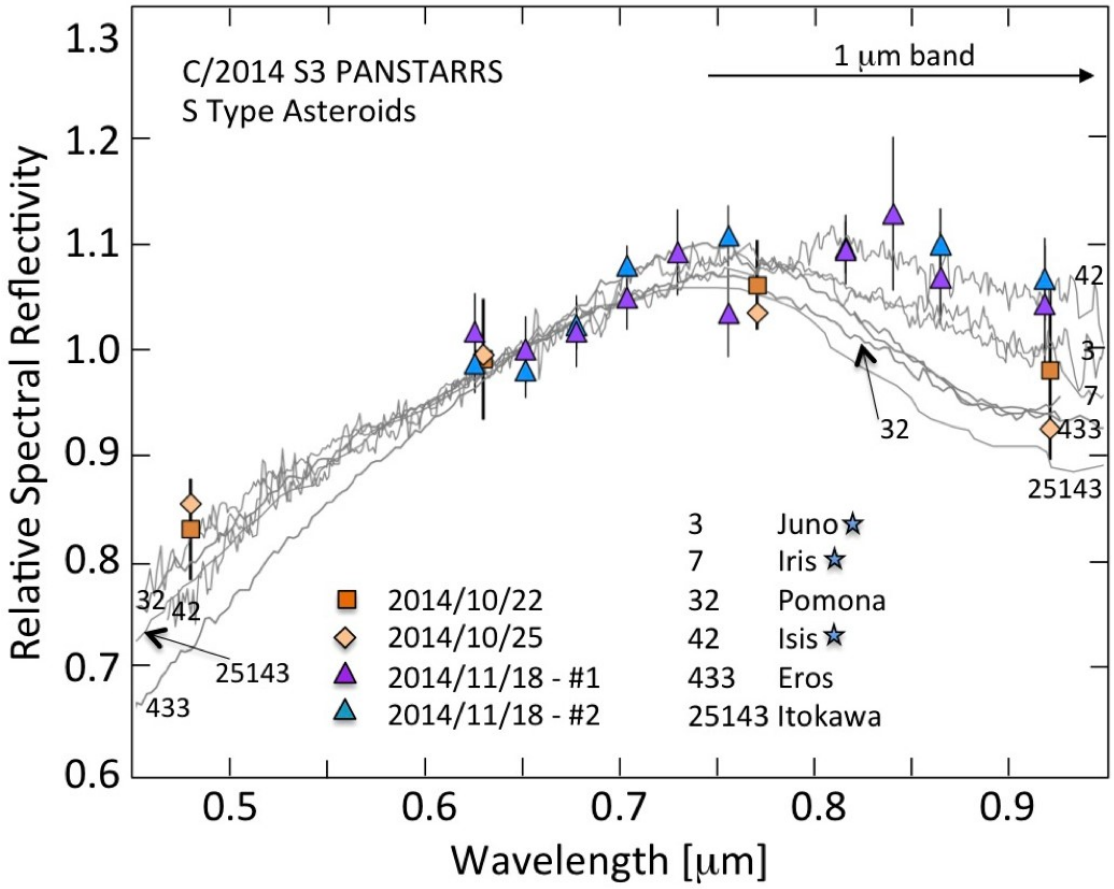

References

[1] Meech, K.J, B. Yang, J. Kleyna, O.R. Hainaut, S. Berdyugina, J.V. Keane, M. Micheli, A. Morbidelli, R.J. Wainscoat, "Inner Solar System Material Discovered in the Oort Cloud", Science Advances, 2016, 2, e16000038

[2] G.R. Huss, et al. in Meteorites and the Early Solar System II, UAZ Press, pp. 567-586

[3] P.M. Doyle, et al. 2015, Nature Comm. 6, 7444

EPSC Abstracts
Vol. 11, EPSC2017-593, 2017
European Planetary Science Congress 2017

Nongravitational effects in the motion of sunskirting comets

V. Emel'yanenko
Institute of Astronomy of the Russian Academy of Sciences, Moscow, Russia (vvemel@inasan.ru / Fax: +7-495-9515557)

Abstract

The orbits of multiple-apparition sunskirting comets 321P, 322P, 323P and 342P have been studied in order to ascertain the significance of nongravitational effects. We assert that nongravitational forces are definitely detectable in the motions of these comets. The nongravitational forces are irregular. There are strong nongravitational accelerations normal to the orbit planes.

1. Introduction

Many of the sunskirting comets with perihelion distances ~ 0.05 au have been observed in several apparitions [1]. In particular, comets 321P, 322P, 323P have been observed in five apparitions, and 342P has been observed in four apparitions. This allows us to study their orbits and to estimate nongravitational effects in their motions.

2. Methods

We determined the orbits of 321P, 322P, 323P and 342P using observations in all the apparitions. The gravitational attractions of all the planets were taken into account, and relativistic terms were included in the equations of motion. From consecutive pairs of the apparitions, we obtained four representations of the observations for 321P, 322P, 323P and three representations of the observations for 342P.

3. Nongravitational effects

From a comparison of the different values for the times of perihelion passage in orbits calculated from different pairs of apparitions, we can detect nongravitational effects in the motion. Nongravitational changes were estimated in 2001, 2004 and 2008 for 321P, in 2003, 2007 and 2011 for 322P, in 2004, 2008 and 2012 for 323P, in 2005 and 2011 for 342P. These computations show that there are nongravitational forces acting on the sunskirting comets. The nongravitational forces are irregular. Differences in the values of orientational elements provide evidence that nongravitational components perpendicular to the orbital planes are substantial. Table 1 shows an example of nongravitational changes for 323P near the perihelion passage in 2012.

Table 1: Changes of the orbital elements (the semimajor axis a, the eccentricity e, the inclination i, the argument of perihelion ω, the longitude of the ascending node Ω, the mean anomaly M) for 323P near the perihelion passage in 2012

Δa, au	0.000049±0.000389
Δe	0.000153±0.000040
Δi, deg	-0.1488±0.0528
$\Delta\omega$, deg	0.7023±0.2179
$\Delta\Omega$, deg	-1.3008±0.2192
ΔM, deg	0.0008±0.0004

Potential interpretations of detected nongravitational variations are discussed. In particular, comparisons are made with the results obtained in [2] for the Kreutz sungrazing system's dwarf comets.

Acknowledgements

This work was supported by the Russian Foundation for basic Research (Grant 16-02-00805).

References

[1] Battams, K. and Knight, M.: SOHO comets: 20-years and 3,000 objects later, Philosophical Transactions A, 2017, in press.

[2] Sekanina, Z. and Kracht, R.: Strong erosion-driven nongravitational effects in orbital motions of the Kreutz sungrazing system's dwarf comets, Astrophysical Journal, Vol. 801, article id. 135, 19 pp., 2015.

EPSC Abstracts
Vol. 11, EPSC2017-738, 2017
European Planetary Science Congress 2017

Cometary dust dynamics and polarization in electromagnetic radiation fields

J. Herranen (1), J. Markkanen (1), and K. Muinonen (1,2)
(1) University of Helsinki, Finland (2) Finnish Geospatial Research Institute FGI, National Land Survey, Finland
(joonas.herranen@helsinki.fi)

Abstract

In this work, we study the polarization of aligned dust particles. The alignment is determined as the stable solution of dynamics due to scattering interactions. The alignment is found to affect on the linear polarization particularly in the 90° scattering angle and backscattering regimes and also induce a measurable circular polarization.

1. Introduction

The observed polarization of cometary comae is due to scattering from asymmetrical dust particles. The alignment of the dust particles is known to alter the polarization. In the context of interstellar dust, it has been firmly established that the dominant alignment method in many situations is by radiative torques.

Due to the modern advancements of different scattering solutions, mainly of the integral equation methods, a complete dynamical scattering solution for arbitrary geometries without orientation averaging is possible with tolerable computational efforts. Computing the T-matrix of scattering with these methods allows the study of dynamical effects of scattering for arbitrary geometries.

In this work, we analyse the polarization of several oriented dust particles. The orientation of the particles is assumed to be due to scattering interactions. Oriented states are found by explicitly integrating the dynamical state of a stationary particle.

2. Methods

We use the electric-current-volume-integral-equation method [2] to calculate the T-matrix of an arbitrary inhomogeneous test geometry [3]. The chosen method provides numerically robust solutions for strongly inhomogeneous scatterers.

The forces and torques due to scattering interactions are calculated from the total electric and magnetic fields, which are presented as vector spherical wavefunction (VSWF) expansions. The fields are related to a mechanical force and torque via the Maxwell stress tensor. The integrals involved can be solved analytically in terms of VSWFs, speeding the force calculations considerably [1].

We model the radiation environment as a discrete blackbody spectrum, with T_{bb} = 5800 K. The cometary dust is modelled as a layered Gaussian random sphere (GRS) [4]. The permittivity of the outer shell is ε_r = 1.95 + i0.786 and of the cores $\varepsilon_r = 1.69 + \mathrm{i}1.04 \cdot 10^{-4}$, modelling silicate cores covered with a carbon layer.

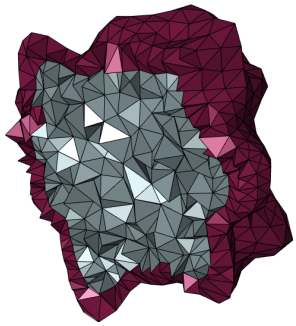

Figure 1: Layered GRS geometry, used to model small solid dust particle.

3. Results

We determined the dynamical evolution of the test geometry, illustrated in Fig. 1, under the radiation of the Sun. The volume equivalent radius of the particle was $a = 200$ nm. The radiation spectrum was a 10-point discretization of the blackbody spectrum between $200 - 2000$ nm. The energy flux of the radiation corresponds to solar irradiance of $330\,\mathrm{Wm}^{-2}$.

The scattering rapidly changes the dynamical state of the particle. Aligned orientation is taken from the state, where the particles angular velocity direction oscillates in a stable manner. The aligned average is then

taken as the average about the angular velocity vector over a single rotation. Polarization results for unpolarized incident light over the discrete wavelength spectrum are illustrated in Fig. 2 for the randomly oriented case, and for two scattering planes in the aligned case. The first scattering plane contains the major principal axis of the particle, and the second scattering plane is perpendicular to the first.

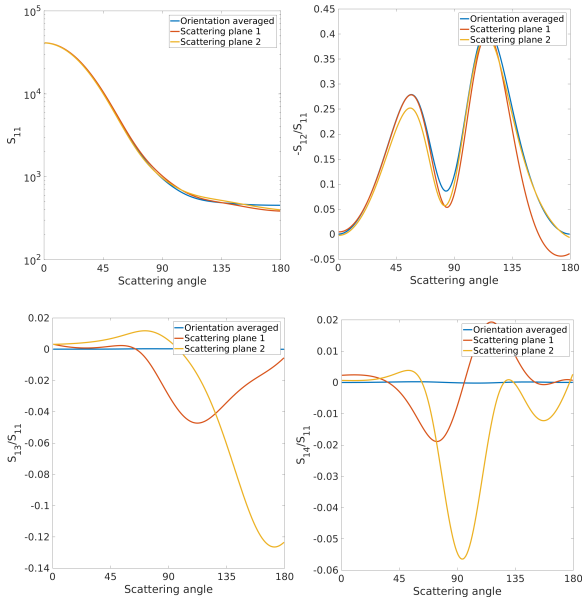

Figure 2: Polarization of randomly oriented and aligned particles. Alignment measurably affects both linear polarization and circular polarization.

4. Conclusions

The scattering forces and torques are significant on the modeled dust particle, leading to rapid alignment. The polarization results of a single test geometry imply encourage systematic study of differently shaped and sized dust particles. Combining the force and torque calculations can also be used to model particle drift in the coma. In the future, this can be used to dynamically model the coma polarization.

Acknowledgements

This work is partly funded by ERC grant 320773 and Academy of Finland grant 1298137.

References

[1] Ø. Farsund and B. Felderhof. Force, torque, and absorbed energy for a body of arbitrary shape and constitution in an electromagnetic radiation field. *Physica A: Statistical Mechanics and its Applications*, 227(1-2):108–130, 1996.

[2] J. Markkanen, P. Ylä-Oijala, and A. Sihvola. Discretization of the volume integral equation formulation for extremely anisotropic materials. *IEEE Transactions on Antennas and Propagation*, 60(11):5195–5202, 2012.

[3] J. Markkanen and A. Yuffa. Fast superposition T-matrix solution for clusters with arbitrary-shaped constituent particles. *Journal of Quantitative Spectroscopy & Radiative Transfer*, 189:181–188, 2017.

[4] K. Muinonen, T. Nousiainen, P. Fast, K. Lumme, and J. Peltoniemi. Light scattering by Gaussian random particles: ray optics approximation. *Journal of Quantitative Spectroscopy and Radiative Transfer*, 55:577–601, 1996.

EPSC Abstracts
Vol. 11, EPSC2017-746, 2017
European Planetary Science Congress 2017

Two-dimensional molecular line transfer for a cometary coma

S. Szutowicz
Space Research Centre Polish Academy of Sciences, Warszawa, Poland (slawka@cbk.waw.pl)

Abstract

In the proposed axisymmetric model of the cometary coma the gas density profile is described by an angular density function. Three methods for treating two-dimensional radiative transfer are compared: the Large Velocity Gradient (LVG) (the Sobolev method), Accelerated Lambda Iteration (ALI) and accelerated Monte Carlo (MC).

1. Model and Summary

Comets exhibit anisotropic gas emission from their nuclei that can be interpreted with non-uniform density distribution models. The main volatile constituent of cometary nucleus ices is water. In the proposed outgassing model, enhanced water emission is related to the discrete active area accompanied by a lower emission of more – uniformly - distributed material. The gas density profile is described by an angular density function.

For radiative transfer calculations the cometary coma is discretized into cells according to spherical coordinate system (r, β) where β is the latitude. A model of excitation of the cometary water molecule includes collisional excitation and infrared pumping by solar radiation. The fractional populations of water rotational levels are derived as simultaneously solution of equations of statistical equilibrium and the equation of radiative transfer in the iterative process. Three methods for treating radiative transfer in the cometary coma are adopted: the Large Velocity Gradient (LVG) (the Sobolev method), Accelerated Lambda Iteration (ALI) and accelerated Monte Carlo (MC). In the LVG method, the radiative transfer is solved locally, and in the ALI and MC methods the radiative energy is transported from one region to the next. In contrast with MC method, in ALI the sampling of the radiation field is not random and is based on a fixed set of long characteristics (LC). ALI and MC agree very well but computational cost of the ALI code is much more lower than MC.

Effects of the physical parameters of the cometary material like density, temperature, and expansion velocity on the line intensity are discussed. The results of simulations for two-dimensional (axisymmetric) density structures are compared; e.g. the population distribution of water rotational levels as a function of distance to nucleus, synthetic line profiles.

EPSC Abstracts
Vol. 11, EPSC2017-781, 2017
European Planetary Science Congress 2017

Photometry as indicator of comets' surface roughness

A. Longobardo (1), E. Palomba (1,2), F. Capaccioni (1), M. Ciarniello (1), F. Tosi (1), S. Mottola (3), L. Moroz (3,4), G. Filacchione (1), A. Raponi (1), E. Quirico (5), A. Zinzi (2,6), M.T. Capria (1,2), D. Bockelee-Morvan (7), S. Erard (7), C. Leyrat (7), G. Rinaldi (1), F. Dirri (1)
(1) INAF-IAPS, via Fosso del Cavaliere 100, 00133 Rome, Italy (andrea.longobardo@iaps.inaf.it); (2) ASI-ASDC, Rome, Italy; (3) DLR, Berlin, Germany; (4) University of Postdam, Postdam, Germany; (5) Université Grenoble Alpes, CNRS, Grenoble, France; (6) INAF-OAR, Rome, Italy; (7) LESIA, Meudon, France

Abstract

We study the photometric behavior of the 67P/Churyumov-Gerasimenko comet by means of Rosetta/VIRTIS data. Comparison with other comets and among different regions of 67P/CG shows a relation between steepness of phase function and surface roughness.

1. Introduction

The VIRTIS imaging spectrometer [1] onboard the ESA/Rosetta spacecraft mapped the surface of comet 67P/Churyumov-Gerasimenko (CG), revealing a dark nucleus (geometric albedo is 0.06 at 0.55 μm [2]) and a widespread occurrence of opaque minerals associated with organic macromolecular materials [3]. Different morphological units have been identified on the comet surface [4], and a link between morphological and spectral properties has been identified [5].
In this work we study the photometry of the Churyumov-Gerasimenko comet, of its macro-regions (i.e. head, neck, head and bottom [4]), and the phase function variation across the surface, in particular between smoother and rougher regions. The obtained results are then compared with phase functions of other comets explored by space missions.

2. Method

Retrieval of phase function is based on the same approach used for Vesta [6], and currently applied on Ceres [7], i.e. a statistical analysis of the VIRTIS dataset. In particular, we considered Pre-Landing data, only, in order to avoid influence of cometary activity in the retrieval of the photometric properties.
Median values of reflectance at different phase angle bins were retrieved and fitted with a polynomial curve, to obtain phase functions at several wavelengths (for simplicity, here we show only results at 0.75 μm, but behavior is similar in the entire visible and NIR spectral range).
Phase function can be described by defining two parameters: R30, i.e. the retrieved reflectance at 30° phase angle, and PCS (Phase Curve Slope), i.e. the steepness of the phase function between 20° and 60° phase angle [8].
We calculated phase functions, R30 and PCS for the entire comet, for the four macro-regions and for specific regions of 67P/CG.

3. Results

The phase function of the Churyumov-Gerasimenko comet and of its four macro-regions are very similar and overlap within errors (Figure 1).

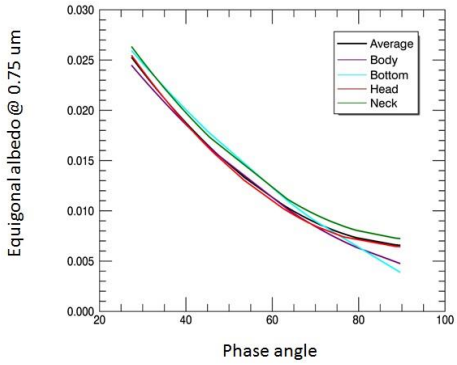

Figure 1. Phase functions of the 67P/CG average and its four macro-regions

The R30-PCS scatterplot including asteroids and comets currently explored by space missions (including 67P/CG) is shown in Figure 2.
Among comets, only Wild2 follow the anti-correlation trend (blue curve) between the two parameters, whereas the other comets show a PCS lower than expected (Table 1). In particular, the PCS is minimum for Churyumov-Gerasimenko.

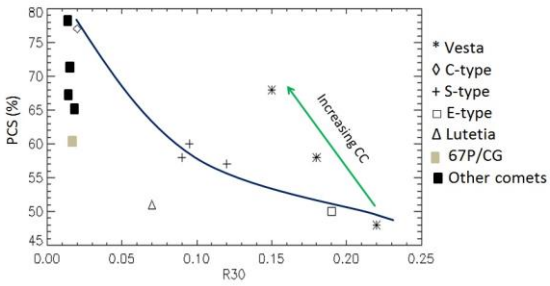

Figure 2. PCS vs R30 scatterplot for asteroids and comets explored by space missions.

4. Conclusions

Since R30 does not vary among comets, the different photometric behaviour of comets should be ascribed to different physical properties, rather than to optical ones.

According to [9] and [10], comets showing higher PCS (i.e. Wild2 and Tempel1) are rougher bodies, whereas 67P/CG shows on average a smoother surface. In order to verify this link between photometry and roughness, we calculated the PCS for 67P/CG surface regions belonging to different morphological classes.

We obtained that PCS of rougher regions (e.g., Anuket and Ash) is larger than the 67P average (67% and 64%, respectively against 60%). On the other hand, in smoother regions (Hapi and Imhotep), PCS is 58% and 55%, hence below the 67P average. A summary of PCS calculated on comets and on specific 67P regions is shown in Table 1.

The observed trend seems to suggest that morphology affects not only spectral properties, as found by [5], but also photometric ones.

Comet/region	PCS
Wild 2	78%
Tempel 1	71%
Hartley 2	67%
Borrelly	65%
Churyumov-Gerasimenko (average)	60%
Anuket	67%
Ash	64%
Hapi	58%
Imhotep	55%

Table 1: PCS of comets and 67P/CG regions.

Acknowledgements

The authors thank ASI, CNES, DLR, NASA for supporting this research. VIRTIS was built by a consortium formed by Italy, France and Germany. Team is leaded by INAF-IAPS and includes LESIA and DLR. The authors wish to thank the Rosetta Science Ground Segment and the Rosetta Mission Operations Centre for their continuous support.

References

[1] Coradini, A. et al. (2007), SSR 128, 529-559

[2] Ciarniello, M. et al. (2015), A&A, 583, id. A31

[3] Capaccioni, F. et al. (2015), Science 347, 6220

[4] Thomas, N. et al. (2015), Science 347, 6220, aaa0440

[5] Filacchione, G. et al. (2016), Icarus 274, 334-349

[6] Longobardo, A. et al. (2014), Icarus 240, 20-35

[7] Longobardo, A. et al. (2017), EPSC abstract, Dawn session

[8] Longobardo, A. et al. (2016), Icarus 267, 204-216

[9] Basilevski, A.T. and Keller, H.U. (2006), PSS 54, 8, 808-829

[10] Ip, W.-H. et al. (2016), A&A 591, A132

EPSC Abstracts
Vol. 11, EPSC2017-877, 2017
European Planetary Science Congress 2017

A dynamical study on extrasolar comets

B. Loibnegger (1) and R. Dvorak (1)
(1) Department of Astrophysics, University of Vienna, Vienna, Austria (birgit.loibnegger@univie.ac.at)

Abstract

Since the detection of absorption features in spectra of β Pictoris varying on short timescales it is known that comets exist in other stellar systems ([1]). In our work we assume the existence of an Oort Cloud like structure around other stars with planetary systems. Collisions of the comets with the planets, close encounters and captures can occur. The different architecture of the systems plays an important role in the outcome of the scattering process, which is why we chose two differently build systems, namely HD 10180 and HIP 14810 for our investigations. We show the influence of the most massive planet on the orbit of captured comets respectively on the collision frequency with the planets and statistics of stable orbits of comets and find that the orbital properties of the most massive planet in the system indeed have an influence on the interaction with the small bodies.

1. Introduction

Evidence for cometary activity in other planetary systems was first found in the analysis of spectra of β Pictoris (e.g.,[1, 6]). They found a large number of metallic absorption lines varying on short time scales which were interpreted as clouds of gas and dust obscuring the light of the star produced by so called falling evaporating bodies. Observations of other star systems yielded the same absorption features, as for example HD 21620, HD 42111, HD 110411, and HD 145964. These transient absorption features were discovered around mainly young ($\sim$ 5 Myr) A-type stars during a campaign by Welsh and Montgomery ([9]) and showed radial velocities in the range of $\pm$ 100$\mathrm{km\,s^{-1}}$. Nilsson et al. (2010) observed 22 exo-Kuiper-belt candidates in five exo-systems and they argue that leftover planetesimal belts are common since dust has a limited lifetime, and observations which proof its existence lead to the assumption that there are larger asteroidal and/or cometary bodies that continuously renew the amount of dust and form dusty debris disks through collisions ([7]).

The study of exocomets is also closely related to the possible habitability of terrestrial planets in extrasolar systems, as comets are able to deliver both liquid water and basic organic substances from regions beyond the snowline to the inner parts of planetary systems (see for example observational results for the Solar System comet 67P/Churyumov-Gerasimenko based on Rosetta (e.g., [8]).)

2. Method and Setup

In order to answer questions about the dynamics of comets in extrasolar systems we did massive n-body calculations with induced thousands of massless cometary bodies dispersed in a sphere around the planetary systems. The n-body calculations have been done with the Lie-Integrator [5] with the planets treated as point masses and the ability of treating close encounters of the comets with the planets with very high accuracy due to the adaptive step-size control. The used systems HD 10180 and HIP 14810 were chosen from *http:// exoplanet.eu/* because of their differences in architecture. HD 10180 is a Sun-like star with 1.06 $\pm$ 0.05 M_{Sun} and has 6 confirmed planets with the most massive one, HD 10180 h, orbiting outside of all the others. HD 10180 h has a mass of 0.21 $M_{Jupiter}$ and semi-major axis of 3.4 AU. HIP 14810 has m = 0.99 $\pm$ 0.04 M_{Sun}. Its planetary system is built the other way round: the most massive planet HIP 14810 b (m = 3.88 $M_{Jupiter}$) at $\sim$ 0.07 AU, with the less massive two other planets orbiting outside of it. The comets stemming from an Oort Cloud like structure around the systems are assumed to have been disturbed by a passing star long time ago and are on their way inward towards the central star on nearly hyperbolic orbits [3, 4]. The comets are started evenly distributed in a spherical structure extending from 90 to 150 AU in the system of HD 10180 and semi-major axis of initially between 30 to 80 AU for HIP 14810 with an eccentricity between 0.91 and 0.99. Integrations of the systems were carried out for a total time of 1 Myr.

3. Results

Due to interactions with the planets comets could either be ejected from the system or stay in the system ("capture"). We show the number of comets ending up in close in stable orbits after the 1 Myr of computations for the two systems according to the initial inclination (see fig1). One can observe that for the system of HD 10180, where in general the planets are farther away from the star, the capture on orbits with low values of eccen- tricity and semi-major axis is only possible for comets with low inclination with respect to the orbital plane of the system. For HIP 14810 captures happen for all inclinations of the comets.

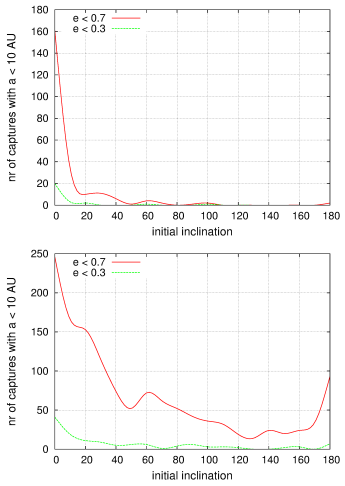

Figure 1: The upper panel shows the number of comets captured on orbits with low eccentricity and semi-major axis for the system HD 10180 ($a_{inital,comet}$= 90AU). The lower panel shows the same for HIP 14810 ($a_{inital,comet}$= 50AU). In the system of HIP 14810 captures are possible for all initial inclinations of the comets.

4. Summary and Conclusions

We can conclude, that the architecture of the system has an influence on the interaction of the planets with the comets. The main influence on the encounter and capture frequency is the value of the semi-major axis of the planets. The closer in a planets orbits, the faster it is and thus the more close encounters with comets it suffers. With collisions it seems to be the other way round. The outer a planet orbits from the star, the more collisions with comets it experiences. This is the same for both systems shown in this study. Nevertheless collisions and encounters are more probable to happen with comets with low initial inclination. For planets farther out this is even more important, as we could observe, that for the closely packed system of HIP 14810 captures of comets is possible for almost all initial inclinations.

Acknowledgements

B.L. and R.D. wish to acknowledge support by the FWF Austrian Science Fund project S11603-N16.

References

[1] Beust, H., Vidal-Madjar, A., Ferlet, R., & Lagrange-Henri, A.-M.: The inner part of the protoplanetary disk around Beta Pictoris, ESA Special Publication, p315, 1990.

[2] Dones, L., Brasser, R., Kaib, N., & Rickman, H.: Origin and Evolution of the Cometary Reservoirs, Space Science Reviews, Volume 197, Issue 1-4, pp. 191-269, 2015.

[3] Duncan, M. J., Brasser, R., Dones, L., & Levison, H. F.: The Role of the Galaxy in the Dynamical Evolution of Transneptunian Objects, The Solar System Beyond Neptune, p.315-331, 2008.

[4] Fouchard, M., Froeschlé, C., Rickman, H., & Valsecchi, G. B.: The key role of massive stars in Oort cloud comet dynamics, Icarus, Volume 214, Issue 1, p. 334-347, 2011.

[5] Hanslmeier, A., & Dvorak, R.: Numerical Integration with Lie Series, Astronomy and Astrophysics, Vol. 132, p. 203, 1984.

[6] Kiefer, F., Lecavelier des Etangs, A., & Vidal-Madjar, A.: Exocomets in the disk of two young A-type stars, SF2A-2014: Proceedings of the Annual meeting of the French Society of Astronomy and Astrophysics, p. 39-43, 2014.

[7] Nilsson, R., Liseau, R., Brandeker, A., et al.: Kuiper belts around nearby stars, Astronomy and Astrophysics, Volume 518, 15 pp, id.A40, 2010.

[8] Rickman, H., Marchi, S., A'Hearn, M. F., et al.: Comet 67P/Churyumov-Gerasimenko: Constraints on its origin from OSIRIS observations, Astronomy & Astrophysics, Vol. 583, id.A44, 8 pp, 2015.

[9] Welsh, B., & Montgomery, S. L.: Exo-comet Detection in Debris Disks Around Young A-type Stars, American Astronomical Society Meeting Abstracts #221, id. 109.03, 2013.

EPSC Abstracts
Vol. 11, EPSC2017-896, 2017
European Planetary Science Congress 2017

Prospects for detecting water in Main Belt Comets

C. Snodgrass
The Open University, Walton Hall, Milton Keynes, United Kingdom (colin.snodgrass@open.ac.uk)

Abstract

Main Belt Comets (MBCs) are objects with asteroid-like orbits in the main asteroid belt, which demonstrate comet-like appearances. While some of these objects can be explained by collisions between asteroids, which leave trails of debris, the repeated activity of some of the population suggests that their activity is driven by the same process as normal comets. Comets' activity is driven by sublimation of ice as they approach the Sun, with water ice thought to be the major driver at heliocentric distances less than about 3 AU, and activity possibly controlled by more volatile species (such as CO or CO_2) at larger distance. These gasses, or the daughter products that they are dissociated into, are detected in the comae of comets. In MBCs there has not yet been a direct detection of gas that would confirm the idea that they are also driven by sublimation. I will review detection attempts, what the expected level of gas production is, and prospects for detection in the future.

1. Main Belt Comets

MBCs were only recently identified as a population in their own right [1], following the discovery of additional objects like the puzzling 133P/Elst-Pizarro, which was first seen active in 1996 and caused some debate over whether it was a comet or collisional debris. The question has been convincingly settled for 133P, as it has returned to activity after each perihelion passage since its discovery, meaning that sublimation of ice is the only reasonable explanation [2, 3]. Other recent discoveries confuse the picture: While 238P/Read also shows repeated activity and is likely a bona-fide comet [4], other objects with comet-like appearance have been shown to be due to collisions or rotational break up (e.g. [5, 6, 7]). Modelling of the dust morphology can be used to differentiate between tails from comet activity which has lasted for many months, and trails of debris from single events. Repeated activity remains the best evidence we have for the comet-like nature of some of these objects. Ideally we would like direct confirmation that their activity is driven by sublimating ice – this requires detection of a gas coma.

2. Searching for gas

For normal comets direct spectroscopy reveals the presence of the gas and allows it to be identified. Water is found to be the main constituent of comets, which is split into OH and H by interaction with sunlight; a strong signature of emission by OH at 308 nm is seen in comet spectra (water itself is very difficult to detect from the ground due to Earth's atmosphere). The next strongest feature in comet spectra is normally the group of CN lines around 389 nm, which are far easier to observe, as the OH line is strongly affected by terrestrial atmospheric absorption, so it is difficult to detect from the ground. For this reason, ground based spectroscopy of MBCs to date has concentrated on the CN band, but has proven unsuccessful (e.g. [8, 9, 10]). The upper limits on water production resulting from these works are inconclusive – the authors assume a 'typical' CN:H_2O ratio based on traditional comets, and use this to derive a limit based on the CN non-detection. Unfortunately, the resulting limits are above the level expected for MBCs based on the observed dust production (MBCs are very weakly active comets), and also the underlying assumption, that MBCs have the same proportions of volatile ices to other comets, is likely to be incorrect. Modelling of the survival of subsurface ice within the snow-line indicates that only water ice will survive, and more volatile ices will be lost [11, 12]. The parent ice species for CN in normal comets is not certain, but a strong candidate is HCN, which is considerably more volatile than water (with a sublimation point of 95K), and is not expected to survive in MBCs.

An attempt was made to detect water around MBC candidate 176P/LINEAR using the ESA Herschel space telescope. This telescope operates at thermal infrared wavelengths, and is sensitive to water emission at 557 GHz. Unfortunately, the targeted comet did not return to activity when expected (the observa-

tions were scheduled to coincide with the same near-perihelion point in the orbit that activity was seen at in 2005), and no water was detected [13]. The upper limit on water production rate from these observations, $Q(H_2O) < 4x10^{25}$ molecules s^{-1}, is more sensitive than most of the limits from CN line observations, and would have been sensitive enough to detect water if MBC production rates follow the same empirical relationship to total brightness found for other comets [14]. This is unknown however, given the low level of activity of MBCs, and another approach (assuming a dust-to-gas mass ratio of one) implies that the total expected rate should have been only $2x10^{24}$ molecules s^{-1}. The authors were forced to conclude that it was possible that there was activity below their detection limit, although they did not know at the time that the comet had not returned to visible activity.

Another attempt was made with the Herschel space telescope for P/2012 T1, which was visibly active at the time, but again resulted in only an upper limit to water production of $Q(H_2O) < 8x10^{25}$ molecules s^{-1} [15]. A VLT search was attempted using the X-SHOOTER spectrograph, which covers a wide range of wavelengths from the UV to near-IR. Critically, it is sensitive down to 300nm at the blue end, so can, in principle, detect the OH emission line at 308nm. Other water-related lines (such as the O[I] line at 630nm, and water lines in the NIR) are unfortunately not resolvable, as the relative velocity of the comet was not enough to shift the lines away from terrestrial atmospheric lines at the resolution we used. Unfortunately this search was also unsuccessful, with a similar upper limit on water production to the Herschel observations [16]. Both the Herschel and X-SHOOTER spectra have the advantage that they do not rely on any assumptions on the link between CN and water production, and can in principle detect water (or its daughter products) directly.

3. Future Prospects

As observations with the best current facilities produce only upper limits, and these limits are not very constraining due to the very weak activity levels of MBCs, we must consider what will be required in the future to make detections. The James Webb Space Telescope is expected to be transformational in many areas of astronomy, and this should also be the case for MBCs – it is expected that its excellent sensitivity to faint emissions will enable direct detection of water outgassing [17]. Other possibilities include dedicated searches in the UV, or a variety of proposed space missions. I will describe these various options, and the advantages and disadvantages of various approaches.

Acknowledgements

CS is funded by the UK STFC through a Rutherford fellowship. This work is based, in part, on discussions which took place at the International Space Science Institute (ISSI) in Bern.

References

[1] Hsieh, H. & Jewitt, D. 2006, Science 312, 561

[2] Hsieh, H., et al. 2010, MNRAS 403, 363

[3] Jewitt, D. 2012, AJ 143, 66

[4] Hsieh, H., Meech, K., & Pittichová, J. 2011, ApJL 736, L18

[5] Snodgrass, C., et al. 2010a, Nature 467, 814

[6] Jewitt, D., et al. 2010, Nature 467, 817

[7] Stevenson, R., et al. 2012, ApJ 759, 142

[8] Jewitt, D., et al. 2009, AJ 137, 4313

[9] Licandro, J., et al 2011, A&A 525, A34

[10] Hsieh, H., et al. 2012, AJ 143, 104

[11] Prialnik, D. & Rosenberg, E. 2009, MNRAS 399, L79

[12] Capria M. T., et al. 2012, A&A 537

[13] de Val-Borro, M., et al. 2012, A&A 546, A4

[14] Jorda, L., et al. 2008, ACM meeting, abs #8046

[15] O'Rourke, L., et al., 2013, ApJ 774, L13

[16] Snodgrass, C., Yang, B., & Fitzsimmons, A., 2017, A&A submitted

[17] Kelley, M. S. P., et al. 2016, PASP, 128, 018009

EPSC Abstracts
Vol. 11, EPSC2017-999-1, 2017
European Planetary Science Congress 2017

Modelling of 67P cometary particles dynamic in the vicinity of the Rosetta spacecraft

F. Cipriani (1), N. Altobelli (2), M. Taylor (3), M. Fulle (4), V. Della Corte (5,6), A. Rotundi (5,6)
(1) ESTEC/TEC-EPS, Noordwijk, The Netherlands, (2) ESAC/SCI-ODI, Madrid, Spain, (3) ESTEC/SCI-S, Noordwijk, The Netherlands, (4) INAF, Osservatorio Astronomico, Trieste, Italy, (5) Università Parthenope, Naples, Italy, (6) INAF Istituto di Astrofisica e Plantetologia Spaziali, Rome, Italy (fabrice.cipriani@esa.int)

1. Introduction

The interpretation of a number of Rosetta datasets (e.g. GIADA, COSIMA, MIDAS...), relies on the description of cometary particles dynamic in the close vicinity of the spacecraft (s/c). In particular, the charged particles behaviour in the 3D s/c sheath open to the instrument entrances is complex and has not been described at such scales.
The existence of a warm electrons population (a few 10 eV energy) in the cometary plasma, as revealed during the Rosetta-comet rendez-vous phase, has been driving the s/c potential to negative values typically in the range -1 to -20V, as inferred from RPC measurements [1].
Observation of cometary particles in the 14µm to ~mm range by GIADA [2] and COSIMA [3] allowed to distinguish so called 'compact' particles, of processed materials from the solar nebula, from 'fluffy' aggregates, of more primitive origin. When detected, such particles have been observed to reach the instruments at speeds of ~m/s or less. In particular, it was inferred that fluffy aggregates are disrupted by electrostatic forces in the vicinity of the s/c due to the effects of local plasma, hence resulting in "particle showers" observed by the instruments.

Based on those observations we consider compact particle populations with typical densities of 3kg/m^3 on the one hand and fragments as produced by the disruption of fluffy aggregates in the s/c vicinity with low densities of 1 kg/m^3 on the other hand.

As illustrated in Figure 1, we use simplified numerical models of the Rosetta s/c and surrounding plasma environment to explore the parameter space (q/m, v), from which we derived conditions leading either charged particles to reach the s/c surface and instruments entrances or being repulsed.

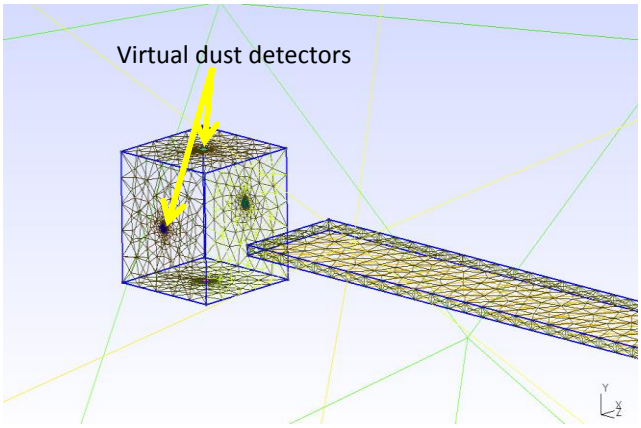

Fig1: Simplified Rosetta numerical model

We use a Particle-In-Cell code adapted to model charged dust in plasmas (the Spacecraft Plasma Interaction Software) to simulate the cometary particles behaviour in the vicinity of the s/c. The s/c potential is fixed to typical values (e.g. -10V for Figures 2, 3 and 4), and the sheath structure is described in terms of plasma densities and potential. In the example of Figure 2 the plasma density was fixed at 200cm^{-3} (T=100eV) and the secondary electrons density is seen to be larger than 500cm^{-3} in the first 10cm of the simplified s/c surface.

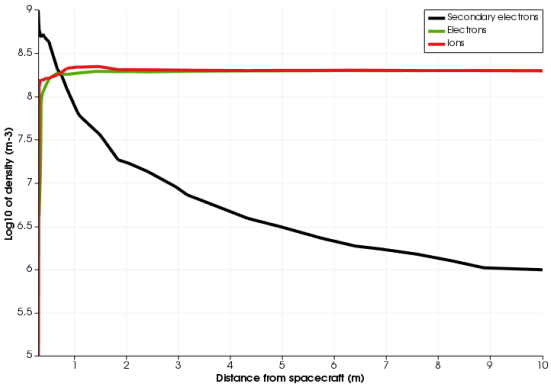

Fig.2: Plasma electrons, ions, and s/c generated secondary electrons profiles within 10m from the centre of the s/c body.

The particles are emitted from a single point or a surface from a distance to the s/c with a distribution of q/m and velocities in the range 1 to 1000m/s. As illustrated in Figure 3, depending on their initial characteristics, some reach the s/c while others are deflected by the s/c potential.

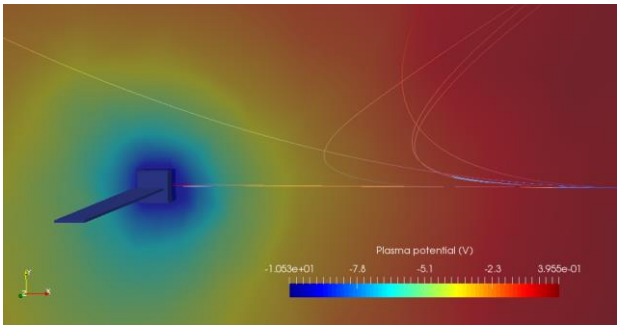

Fig.3: Plasma potential (with Rosetta surface potential fixed at -10V) together with particle trajectories originating from a point source located 8.0m away.

The particles are tracked until they are stopped by the s/c surface or exit the simulation domain boundary. The set of coordinates, velocities, potential and charge as well as plasma electric field and potential are recorded along each trajectory as illustrated in Figure 4.

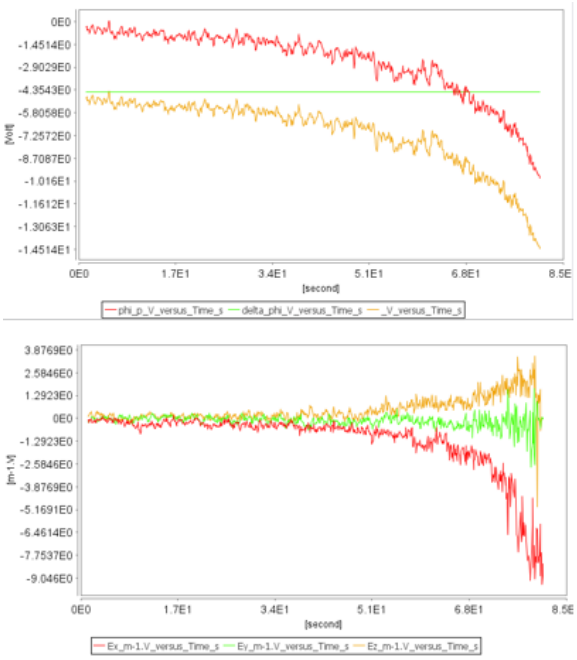

Fig.4: Upper panel: plasma and dust potential along the trajectory from outside the sheath to the s/c surface for a collected particle. Bottom panel: electric field components along the trajectory.

The s/c model is iterated in complexity such as to represent a realistic sheath and instrument entrance geometry, computing time permitting. In the end, we will elaborate on dust particles behaviour in the s/c sheath and measure the dust characteristics at impact on surfaces mimicking instruments entrances (fluxes, velocities, q/m distributions), in order to help the interpretation of Rosetta observations.

References

[1] A. Errikson et al, The Plasma Environment of Rosetta at Comet 67P, Proceedings of the 14th SCTC, Noordwijk, April 2016
[2] M. Fulle et al, ApJL, 802:L12, 2015
[3] S. Merouane et al, A&A, 596, A87, 2015